The Earth's Building Blocks

Frédéric Moynier, Bruce Fegley

To cite this version:

Frédéric Moynier, Bruce Fegley. The Earth's Building Blocks. The Early Earth, 2015, 10.1002/9781118860359.ch2 . hal-01381065

HAL Id: hal-01381065
https://hal.science/hal-01381065

Submitted on 6 Nov 2022

The Earth's building blocks

Frédéric Moynier[1] & Bruce Fegley, Jr.[2]

[1]Institut de Physique du Globe de Paris, Insitut Universitaire de France, Université Paris Diderot, Sorbonne Paris Cité, 1 rue Jussieu, 75238 Paris Cedex 05 [2]Planetary Chemistry Laboratory, Department of Earth & Planetary Sciences and McDonnell Center for the Space Sciences, Washington University, St Louis, MO 63130 USA

Abstract

In this paper we propose an updated bulk chemical composition of the Earth based on new estimates for the composition of the Earth's core. We present the different cosmochemical constraints that allow us to search for the Earth's building blocks. Chemical equilibrium calculations of gas – solid equilibria in solar composition gas show that at first approximation the Earth is chondritic for the refractory lithophile (rock-loving) elements. Elemental and isotopic compositions are then used to discuss the different possible types of meteoritic material (exemplified by the meteorites in our collections) that may represent the bulk Earth composition.

Introduction

Consideration of Earth's building blocks requires knowledge of its bulk composition today, chemistry in the solar nebula, and of chemical effects during accretion of the Earth (e.g., see pp. 35-38 of Lewis & Prinn 1984). The Earth is a differentiated planet consisting of five (physically distinct) geochemical reservoirs (atmosphere, biosphere, hydrosphere, lithosphere, and core) with different chemical compositions. (In this paper we *geochemically* define lithosphere as the crust plus the entire mantle so it encompasses the entire silicate portion of the Earth. This is distinct from the geophysical definition of lithosphere, which is based on mechanical properties of rock.) Thus, the lithosphere is similar, but not identical to the bulk silicate Earth, which also includes the atmosphere, biosphere, and hydrosphere (see below). All accessible terrestrial samples have been modified to a greater or lesser extent from Earth's original composition. For example, the atmosphere, biosphere, hydrosphere, and lithosphere originated from Earth's primordial silicate portion after it was depleted in siderophile (metal-loving) and chalcophile (sulfur-loving) elements by core formation but before it differentiated into crust plus mantle and outgassed volatiles to form the atmosphere and oceans. Thus the mass-weighted chemical composition of the atmosphere, biosphere, hydrosphere, and lithosphere is that of the bulk silicate Earth (BSE), also known as Earth's primitive mantle (PM). We use the term BSE throughout this chapter. Two major processes shaped the composition of the BSE: (1) gas – solid (and/or gas – melt) volatility fractionation of Earth – forming materials in the solar nebula (including volatility effects on planetesimals), and during accretion of the Earth, and (2) silicate, metal, and sulfide elemental partitioning during core formation on the early Earth and its planetesimal precursors.

We could also divide the Earth into geochemically different reservoirs such as undepleted primitive mantle (UPM) and depleted MORB mantle (DMM), but we did not take this approach for two reasons. First, the size of the undepleted and depleted reservoirs may vary for each element and isotope under consideration, e.g., different size reservoirs for a lithophile and a noble gas. Second, the depleted and undepleted reservoirs are model constructs that do not necessarily correspond to physically different reservoirs such as upper and lower mantle. For example the entire mantle may be a mixture of more and less depleted regions like raisins in a cake (Figure 6 of Helffrich & Wood 2001).

It is more convenient for us to consider the five physically distinct reservoirs mentioned above. In principle, Earth's bulk composition can be reconstructed from chemical analyses of elements in each of these five reservoirs combined together in their relative mass fractions. Thus the concentration C of an element E in the bulk Earth (Bulk) is given by

$$C_E^{Bulk} = F_A C_E^A + F_B C_E^B + F_H C_E^H + F_L C_E^L + F_C C_E^C$$

The mass fraction of each reservoir R is F_R and the subscripts denote the atmospheric (A), biospheric (B), hydrospheric (H), lithospheric (L), and core (C) reservoirs. Table 1 lists the mass and mass fraction of each of these reservoirs and shows the further subdivision of the lithospheric and core reservoirs. The concentration of an element E in each reservoir is C_E^R. For example, the bulk earth concentration of Mg is given by

$$C_{Mg}^{Bulk} = F_A C_{Mg}^A + F_B C_{Mg}^B + F_H C_{Mg}^H + F_L C_{Mg}^L + F_C C_{Mg}^C$$

$$C_{Mg}^{Bulk} = (8.6\times10^{-7})(0\%) + (1.9\times10^{-9})(0.098\%) + (2.79\times10^{-4})(0.128\%)$$

$$+ (0.6748)(22.17\%) + (0.3249)(0\%)$$

$$C_{Mg}^{Bulk} = 14.96\%$$

In comparison, Morgan & Anders (1980), Kargel & Lewis (1993), and McDonough (2003) give 13.90%, 14.86%, and 15.4% Mg, respectively, in the bulk Earth. The variations are due to the different values selected for the Mg percentage in Earth's mantle. The amounts of Mg in the atmosphere (none), biosphere (0.098% in phytomass), hydrosphere (0.128% in seawater) (Lodders & Fegley 1998, 2011), lithosphere (22.17%, Table 4 of Palme & O'Neill 2014), and core (none, McDonough 2003) are very small. Thus, the Mg concentration in the bulk Earth is effectively just the mass-weighted Mg concentration in the lithosphere.

We can simply write the mass balance equations by using elemental concentrations in the BSE; then a two-term equation results, e.g., the equation for Mg becomes:

$$C_{Mg}^{Bulk} = F_{BSE} C_{Mg}^{BSE} + F_C C_{Mg}^{C}$$

$$C_{Mg}^{Bulk} = (0.6751)(22.17\%) + (0.3249)(0\%) = 14.96\%$$

Other lithophile elements that are insoluble in water and do not behave as siderophiles or chalcophiles at core-forming conditions (e.g., Al, Ba, Be, Ca, F, Li, REE, Sc, Sr, Th, Ti, U, Y, Zr) have similar mass balance equations comprised of only the lithospheric reservoir term. (We defer discussion of Na, K, Rb, and Cs to later.)

Several other elements are concentrated in one reservoir, but not to the same extent as the lithophiles mentioned above. For example, most of the iodine in the bulk silicate Earth is primarily found in organic-rich marine sediments and marine organisms (i.e., biospheric reservoir) with ~ 11% residing in the lithosphere. However, the core may contain up to 82% of Earth's total iodine inventory if metal/silicate partition coefficients measured at high pressures and temperatures are relevant to core formation on Earth (Armytage et al. 2013).

About 75% of Cl and Br in the BSE are in the oceans (hydrospheric reservoir) with the remaining 25% in the lithosphere. Neglecting any nitrogen that may be dissolved in the molten outer core, 73.1% of Earth's nitrogen is in the atmosphere, 26.5% is in the crust, and 0.4% in the oceans (Lodders & Fegley 2011). Geochemical modeling (Allegre et al. 1995; Albarede 1998; Ballentine & Holland 2008) shows only 45-50% of Earth's ^{40}Ar is in the atmosphere. This modeling depends on the amount of K in the BSE, which is fairly well constrained at 230 – 280 ppm by mass (260 ppm, Jagoutz et al 1979; 240 ppm, McDonough & Sun 1995; 232 ppm, Kargel & Lewis 1993; 258 ppm, Hofmann 1988; 231 ppm, Wänke et al 1984; 258 ppm, Hart & Zindler 1986; 280 ppm, Allègre et al. 1995; and 260 ppm, Palme & O'Neill 2014). If the degassing efficiency is similar for other noble gases, the atmosphere contains ~ 50% of Earth's $^{36+38}$Ar, Kr, and Xe (Fegley & Schaefer 2014). Helium is not considered in this comparison because it is continually escaping to space with an atmospheric lifetime of 0.9–1.8Ma for ^{4}He and 0.4–0.8Ma for ^{3}He (Torgersen, 1989). Neon is not considered because the different isotopic compositions of atmospheric and mantle Ne suggest atmospheric Ne is probably a mixture of Ne degassed from the mantle and from chondritic bolides by impact degassing (Marty 2012; Moreira 2013; Zhang 2014). An alternative scenario is the Ne has been lost by hydrodynamic escape to space associated with an isotopic mass-fractionation (Pepin 2006).

The atmospheric inventory of Xe is lower than it should be by analogy with Ne, Ar, and Kr – the missing Xe problem. Various solutions to the missing Xe problem have been suggested over the past 50 years, which generally involve sequestering the "missing" Xe inside the Earth, e.g., in glacial ice, sediments, or clathrate hydrates (e.g., see Ozima & Podosek 2001). More recently Sanloup et al. (2005, 2011) suggested that significant amounts of Xe are in the lower mantle or in the crust as XeO_2 in quartz and olivine, which is supported by the synthesis of XeO_2 (Brock & Schrobilgen 2011). A last scenario is that Xe has been lost to space through an unknown process associated with an isotopic fractionation (Pujol et al. 2011). Over the past 30 years geoscientists have speculated that the "missing" Xe is in Earth's core (Ozima & Podosek 2001). Their reasoning is that Xe becomes a metal with hexagonal close packed (hcp) structure above 120 GPa and it may alloy with, or dissolve into Fe, which is also a hcp metal at core conditions. However the experimental study of Nishio-Hamane et al. (2010) finds no evidence for Xe alloy formation with or dissolution into Fe at P, T conditions similar to those in the core. A more detailed discussion of noble gas geochemistry is beyond our scope, but is given by Zhang (2014).

As evident from our discussion above, this simple mass balance approach is difficult in practice because of our incomplete knowledge of reservoir compositions, e.g., the core, which is ~ 32.5% by mass, and the mantle, which is ~ 67.5% by mass, of the Earth. For example, recent metal/silicate partitioning experiments indicate that Earth's core may be a significant reservoir of helium (Bouhifd et al. 2013a), iodine (Armytage et al. 2013), and lead (Bouhifd et al. 2013b). The measured partition coefficients depend upon several variables (e.g., P, T, oxygen fugacity, sulfur content of the molten metal) and the "true" concentrations of these and many other elements in Earth's core will be incredibly difficult to constrain. Likewise, the concentrations of several elements in the mantle are not well known, e.g., As, Bi, Cd, H, In, S, Sb, Se, Te, Tl. The estimate of H in the mantle varies from 1 – 2 oceans of water (e.g., Saal et al. 2002, Hirschmann & Dasgupta 2009; Zhang 2014). Even the crustal concentrations of some elements such as As, Bi, Hg, Sb, and Tl are poorly known (Palme & O'Neill 2014).

Our knowledge of the compositions of the five major geochemical reservoirs comes from four principal types of data: (1) seismological observations, (2) chemical and isotopic analyses of the atmosphere, biosphere, hydrosphere, and lithosphere, (3) experimental studies of elemental partitioning between coexisting phases (e.g., metal, silicate, sulfide, melt) as a function of temperature, pressure, oxygen and/or sulfur fugacity, (4) ratios of elements with very similar geochemical behavior (e.g., Sm/Sn, K/U, K/La, W/Th, P/Nd, Rb/Ba, Nb/Ta) combined with analysis of one element in the pair, and (5) cosmochemical constraints, e.g., elemental and isotopic abundances in meteorites and solar composition material.

Palme & O'Neill (2014) describe in more detail several of these approaches that they use to determine the composition of the bulk silicate Earth. Thus we do not repeat their discussion here but refer the reader to their chapter. Published values for composition of the BSE are in good agreement. For example, Table 3 of Palme & O'Neill (2014) compares BSE major element compositions from Ringwood (1979), Jagoutz et al (1979), Wänke et al (1984), Palme & Nickel (1985), Hart & Zindler (1986), McDonough & Sun (1995), and Allègre et al. (1995). The range for SiO_2 – the most abundant oxide in the BSE – is only from 45.0% (McDonough & Sun 1995) to

46.2% (Palme & Nickel 1985) – and the unweighted mean value of all seven compilations is 45.6 ± 0.5% (1 sigma error), identical within error to the value of 45.40 ± 0.30% recommended by Palme & O'Neill (2014). Likewise the concentration range for MgO – the 2nd most abundant oxide in the BSE – is from 35.5% (Palme & Nickel 1985) to 38.3% (Jagoutz et al. 1979). The unweighted mean MgO concentration from all seven compilations is 37.4 ± 0.9% (1 sigma error), identical within error to the value of 36.77 ± 0.44% given by Palme & O'Neill (2014). Table 6.9 of Lodders & Fegley (1998) compares ten BSE compositions, and the same conclusion is reached – that the major element composition of the BSE is well constrained. As we discuss later these BSE compositions assume that the mantle is compositionally uniform. There is good evidence for this summarized by Palme and O'Neill (2014).

More than one line of evidence is often used to constrain the composition of the lithospheric and core reservoirs. For example, seismological observations show the Earth is physically divided (to 1st order) into crust, upper mantle, lower mantle, and core, and that Earth's core is divided into a molten outer core and a solid inner core. Seismic data and analyses of Fe-Ni meteorite metal show that most of the core is Fe-Ni alloy (Fe/Ni ~ 16.5 by weight = Fe 94.3%, Ni 5.7% – this is the solar composition value which is found in most iron meteorites). However, the molten outer core is ~ 5-10% less dense and the inner core is ~ 2-3% less dense than this alloy (Badro et al. 2014). One or more light elements are present in the core (Birch 1952, 1964). The identity of the light element(s) in the molten outer core and in the solid inner core is not uniquely constrained by the seismic data alone but also depends upon observed elemental abundances in Fe-Ni alloy in meteorites, Fe – element binary phase diagrams, metal/silicate partition coefficients, and solar elemental abundances; the plausible light elements include C, S, Si, O, N, P, and H. Molecular dynamics simulations of density and sound speed at plausible P & T for the core by Badro et al. (2014) show oxygen is the most abundant light element in the core with their best fit model containing 3.7% O and 1.9% Si by weight. The maximum light element contents permitted by their modeling are 5.4% O, 4.5% Si, and 2.4% S.

Seismic tomography shows the penetration of down-welling slabs into the lower mantle, which requires mass exchange between upper and lower mantle. This evidence is important because it implies a generally well-mixed, compositionally uniform mantle (Palme & O'Neill 2014). Bina & Helffrich (2014) computed density and sound velocity profiles along plausible lower mantle adiabats for a variety of compositions and concluded that lower mantle physical properties are consistent with a pyrolite, i.e., upper mantle, composition. Palme & O'Neill (2014) review other lines of evidence supporting a homogenous mantle composition.

Thus most geoscientists accept that analyses of relatively unaltered upper mantle xenoliths (fertile peridotites, spinel lherzolites, garnet lherzolites), petrological models of peridotite – basalt melting (e.g., Ringwood's pyrolite model), and concentration ratios of geochemically similar elements in basalts, can be used to determine the composition of the entire mantle – not just the upper mantle. But see Anderson (2002) and Javoy et al. (2010) for arguments that the upper and lower mantle has different compositions. The latter group requires this in order for their enstatite chondrite model to match the BSE.

In this review we focus on three lines of evidence– cosmochemical constraints and geochemical and isotopic analyses– that provide information about the bulk composition of the Earth and its building blocks.

Cosmochemical constraints

We discuss meteoritic constraints on Earth's composition and origin in a subsequent section. Here we discuss constraints from solar nebula chemistry, but before doing so we briefly summarize the different stages of solar nebula evolution, and planetary accretion based on Cameron (1995), Lodders & Fegley (2011), and Chamber (2014).

1st *Stage: Molecular cloud collapse*. During this stage, the solar nebula disk is built up of infalling material from a collapsing molecular cloud core. This stage lasts for a few times 10^5 years. Most (if not all) of the matter in the disk during this stage ultimately goes into the proto-Sun.

2nd *Stage: Disk dissipation*. The Sun forms during this stage, which lasts for about 50,000 years (i.e., the Sun accretes at approximately 2×10^{-5} solar masses per year). The disk mass is less than that of the proto-Sun. Most matter falling onto the accretion disk is transported through the disk into the proto-Sun and angular momentum is transported outward in the disk. The major dissipation (i.e., transport) mechanisms include spiral density waves, disk-driven bipolar outflows, and the Balbus-Hawley magnetic instability. Cameron (1995) discusses why turbulent viscosity driven by thermal convection is less important than these other dissipative mechanisms, but some other modelers continue to rely on turbulent viscosity as the main dissipative mechanism. The amount of outward mass transport, that would tend to "contaminate" the outer nebula with products from thermochemical processing in the innermost few AU of the nebula, is controversial and uncertain. Near the end of this stage, some disk material survived and is preserved in meteorites (e.g., ^{26}Al-bearing minerals).

3rd *Stage: Terminal accumulation of the Sun*. The final accumulation of the Sun occurs during this stage, which lasts for about (1-2) × 10^6 years. The Sun's accumulation rate decreases from about 10^{-7} to 10^{-8} solar masses per year. The proto-Sun becomes a classical T Tauri star in this phase. Planetary accretion (almost complete for Jupiter and Saturn, and less advanced for the other planets) occurs during this stage.

4th *Stage: Loss of nebular gas*. The Sun becomes a weak line T Tauri star in this stage, which lasts (3-30) × 10^6 years, and is no longer accreting material from the disk. The T Tauri wind removes gas in the inner nebula and photo-evaporation due mainly to UV radiation from the T Tauri wind removes gas in the outer nebula. Ultraviolet photochemistry may be important in the outer nebula, but its importance depends on the poorly constrained and time dependent nebular column density. Nebular gas – solid thermochemistry ceases sometime (although not necessarily at the same time everywhere) during this stage.

In Cameron's (1995) model of nebular evolution, accumulation of the Sun consumed essentially all of the material accreted by the nebular disk during the early stages of its history. Planets and all the other bodies in the solar system were then assembled from material accreted after the Sun had formed (i.e., during the time from the end of stage 2 into stage 4). Accretion of the terrestrial planets proceeded via a multistage process of planetary embryo growth from nebular dust grains (dust grains → chunks → boulders → km size bodies → asteroidal size bodies → planetary embyros → planets). The number of objects decreased at each stage of accretion until roughly a few hundred planetary embryos of lunar to Mars size are produced. The four terrestrial planets formed by accretion of these planetary embryos. For example, the last stage of Earth accretion apparently involved collision of the ~ 0.9 M_E proto-Earth with an ~ 0.1 M_E Mars-size body.

The composition of the dust grains that were the starting point for planetesimal growth and accretion was mainly determined by nebular thermochemistry; thus we discuss constraints on chemistry of nebular solids from chemical equilibrium calculations of gas – solid equilibria in solar composition gas. Prinn & Fegley (1989) showed thermochemistry was the dominant chemical process in the inner solar nebula where the terrestrial planets formed. At 1 AU they found thermochemistry is 10 times more important than shock chemistry, 40,000 times more important than photochemistry, and over 13 million times as important as radiochemistry. For example, absorption of UV radiation by water vapor (the third most abundant gas in the solar nebula after H_2 and He) and scattering by dust dramatically decreases the Ly-α photon flux from the proto-Sun at 1 AU. Hotter, denser conditions inward of 1 AU in the solar nebula made thermochemistry even more important closer to the proto-Sun. This is also due in part to increased abundances at higher temperatures of CO and UV absorbing gases of rock-forming elements (e.g., SiO, SiS, HS, H_2S, AlOH, Al_2O, AlS, AlH, AlO, PO, PN, PS, NaCl, HCl, KCl, KOH, TiO, and TiO_2) that are thermodynamically stable in the inner region of the solar nebula (e.g., see Table 2 and Figures 1-17 of Schaefer & Fegley 2010b). Some of these gases absorb UV light at the same wavelengths as H_2O and others absorb at shorter (e.g. CO, SiO) or longer wavelengths (e.g., H_2S). Methane, CO_2, and NH_3 become more abundant and contribute to UV opacity of the solar nebula at a few hundred Kelvin where the CO – CH_4 (625 K at 10^{-4} bar total pressure) and N_2 – NH_3 equal abundance lines (345 K at 10^{-4} bar total pressure) are reached (e.g., see Figures 14-15 in Schaefer & Fegley 2010b). With decreasing temperature below the equal abundance lines, CH_4 and NH_3 become more important until they are the major C- and N-bearing gases. The UV opacity due to all of the gases listed above vanishes once the respective elements condense. For example at 10^{-4} bar total pressure Si is 50% in the vapor as SiO and SiS and 50% condensed as forsterite plus enstatite at 1310 K. The UV opacity due to H_2S persists to much lower temperatures because sulfur is 50% condensed as FeS at 664 K. The UV opacity due to water vapor persists until low temperatures of $\sim$ 180 K (10^{-4} bar total pressure) where 50% of H_2O is in the vapor and 50% is condensed as water ice. At 10^{-4} bar total pressure, ammonia condenses as NH_4OH (131 K) and CH_4 as CH_4 clathrate hydrate at 78 K. Thus all of the gaseous UV opacity sources – except for CO – should be absent from the outermost solar nebula.

In contrast, chemical modeling of protoplanetary disks by astronomers (e.g., Henning & Semenov 2013) uses chemical kinetic codes and focuses on lower temperature, lower density disk regions that are “thin” to electromagnetic radiation (e.g., R ≥ 10 AU beyond the condensation fronts for molecules such as H_2O that absorb UV radiation). Indeed, the calculations of Prinn & Fegley (1989) showed that stellar UV photochemistry is important in these outer nebular regions (see pp. 85-92 of their paper). For example, the CO photochemical models of Lyons and Young (2005) for production of oxygen isotopic anomalies are done at 30 AU and require a far UV flux about 10^3 times larger than the local interstellar medium. But as mentioned earlier, we are interested in the higher temperature, higher density inner disk regions that are opaque (hence convective), where chemical equilibrium is reached within the disk lifetime.

In the next 10 – 20 years we can expect quantitative information about the composition of protoplanetary disks from ALMA (Atacama Large Millimeter/ submillimeter Array), JWST (James Webb Space Telescope), and other telescopes. Ultimately we may have good constraints on the composition of the dust and gas as a function of radial distance in the solar nebula from astronomical observations of solar metallicity protoplanetary disks, but at the present time we must rely on chemical equilibrium models.

Until the discovery of planets and planetary systems around other stars (exoplanets) it was generally believed that the Earth formed at about its present location from the Sun. However, many of the exoplanets discovered to date are gas giant planets very close to their parent stars (e.g., see the catalog at exoplanet.eu). The accepted model for formation of these extrasolar gas giant planets involves formation at much larger radial distances and radial migration inward to their present positions (Perryman 2011). Thus it may be possible that the Earth also formed much farther outward of its present position and migrated inward to one astronomical unit (AU; 1 AU = Earth's average distance from the Sun), e.g., as in the giant gaseous protoplanet models of Cameron and colleagues (DeCampli 1978; DeCampli & Cameron 1979; Slattery 1978). We cannot rule out this model definitively but we think it is extremely unlikely for two reasons. First, formation of the Earth from a giant gaseous protoplanet that has migrated inward to 1 AU involves the loss of large amounts of H_2, He, other noble gases, water, and C-bearing compounds. For example, a solar composition giant gaseous protoplanetary Earth (with 14.96% Mg in the "rocky + metallic" portion as in the bulk Earth) would have to lose ~ 180 Earth masses (M_E) of H_2, ~ 60 M_E of He, and ~ 2.7 M_E of Ne, H_2O, N-, and C-compounds (~ 243 M_E total) to get to its present composition. Second, calculations by DeCampli & Cameron (1979) show that a giant gaseous protoplanet rapidly collapses to a state where removal of light elements (H, He) is impossible within the lifetime of the solar nebula. As a result the formation of the Earth by sedimentation of condensed material within the giant gaseous protoplanet leads instead to a Jovian planet rich in H and He (Slattery 1978; Slattery et al. 1980). It may be interesting to explore the chemistry of giant gaseous protoplanets for application to rocky exoplanets with H_2-bearing atmospheres in other planetary systems. However these models seem irrelevant to formation of the Earth and thus our discussion assumes the Earth formed at 1 AU and accreted material at about this location.

Figures 1 and 2 show the chemical equilibrium calculations of Barshay (1981) given as condensate abundances versus inverse radial distance (1/R) from the proto-Sun in astronomical units. These calculations are done for a convective solar nebula model with an adiabatic temperature – pressure profile with these characteristics: T_o = 600 K, P_o = 10^{-4} bar, R_o = 1 AU. The variation of temperature with radial distance and pressure with temperature in the midplane of the nebula are given by (Lewis 1974)

$$\frac{T}{T_o} = \left(\frac{R}{R_o}\right)^{-1.1}$$

$$\frac{P}{P_o} = \left(\frac{T}{T_o}\right)^{C_P/R}$$

To first approximation the details of this model are irrelevant because (1) the condensation sequence is relatively insensitive to total pressure (see Fig 1 in Lewis 1974; Fig 3.8 in Lodders & Fegley 2011) and (2) other models of the solar nebula accretion disk give the same basic result – T and P decreasing with increasing radial distance from the proto-Sun (e.g., Fig 3.5 in Lodders and Fegley 2011).

The major conclusion from Barshay's chemical equilibrium calculations is that the Earth-forming material at 1 AU should have chondritic relative abundances of rock-forming "metals" (e.g., Mg, Si, Fe, S, Ni, Al, Ca, Na, K, Ti) because compounds of these elements are fully condensed at higher temperatures (smaller radial distances) from the proto-Sun (see the discussion of accretion functions below). His calculations did not include other minor and trace elements (e.g., Cr, Mn, P, Co, refractory lithophiles, refractory siderophiles) that are fully condensed at 600 K in the solar nebula but based on other calculations (e.g., Larimer 1967; Grossman &

Larimer 1974; Lewis 1972; Lodders 2003) we know which elements are fully condensed by 600 K, 10^{-4} bar, 1 AU. Barshay's main result thus agrees with arguments of other geoscientists that Earth is chondritic to *first approximation* in major element chemistry (e.g., Wänke 1981; Kargel & Lewis 1993; Palme & O'Neill 2014). His results predict a CI chondritic Mg/Si ratio of 0.90 for the Earth (vs. 0.92 in our model in Table 2), which is not the case unless significant amounts of Si are dissolved in the core.

It is likely that the original composition of solids condensed in the solar nebula was altered – to a greater or lesser extent - as accretion proceeded and grains eventually grew into planetesimal-size meteorite parent bodies. Aqueous alteration, dry thermal metamorphism, and shock metamorphism are evident in various types of chondritic meteorites. For example, thermal metamorphism on meteorite parent bodies altered the chondrites in our meteorite collections. Originally, chondritic material was plausibly more volatile-rich than even the most volatile-rich ordinary chondrite samples in meteorite collections today. The larger volatile abundances in the unequilibrated ordinary chondrites (i.e., the H3, L3, LL3 chondrites), which are less metamorphically altered than the grade 4–6 ordinary chondrites, support this argument (Schaefer & Fegley 2007). However, it is also known that even the extensive aqueous alteration on the CI chondrite parent body did not alter their elemental abundances even though their mineralogy was changed (e.g., Anders & Grevesse 1989; Lodders 2003).

The question of how collisions may have altered planetesimal compositions is important, but not yet answered. On the one hand collisional mixing is evident in our meteorite collections through the presence of “meteorites in meteorites” – xenoliths of one type of meteorite enclosed in another (Wilkening 1977). On the other hand, the “meteorite in meteorite” samples are the exception rather than the rule. Collisions between large bodies, such as the lunar to Mars size planetary embryos that are believed to have formed the terrestrial planets are very energetic. For example, extensive melting and partial vaporization may have occurred on the post Giant Impact Earth (Lupu et al. 2014; Fegley & Schaefer 2014), but the amount of “volatiles” lost from the post-impact Earth is poorly constrained, and may have been small because of Earth’s large escape velocity (e.g., see Genda & Abe 2003a, 2005; Pahlevan 2010; Lupu et al. 2014). Even hydrodynamic escape of vapor from the proto-lunar disk is problematic because of the strong gravity field (Genda & Abe 2003b).

Collisional erosion is another process suggested to alter composition of planetary embryos by loss of the outer layers, perhaps early formed crust, on the embryos (e.g., O’Neill and Palme 2008). These new models are motivated in part by the ^{142}Nd excess in terrestrial samples (e.g., Boyet & Carlson 2005; Caro & Bourdon 2010) but as argued by Huang et al. (2013) the observed excesses are within the range of observed ^{142}Nd variations in chondritic meteorites. Another motivation is the high metal to silicate ratio of the planet Mercury. In this case the geochemical analyses by the MESSENGER spacecraft support the idea that much of its silicate portion was lost by collisional erosion (e.g., see Cameron et al. 1988 for a discussion of alternative models for producing Mercury’s high metal to silicate ratio). Excluding the planet Mercury, we conclude that at present we simply do not know how collisions of planetary embryos altered their chemical compositions.

What is clear is that the terrestrial planets accreted material formed over a range of radial distances in the solar nebula. Barshay (1981) modeled this process by convolving his nebular chemistry calculations with simple accretion functions (e.g., square wave, triangular, Gaussian) with variable widths defined by the full width at half maximum (FWHM = 0.06 – 0.60 AU^{-1}). This may have been the first attempt to combine a model of solar nebula chemistry with a model of planetesimal accretion. Barshay (1981) used accretion functions of different geometric shape and size as a proxy for planetary accretion from smaller planetesimals over a range of radial distances (Figure 3 – 5). For example, if Earth collected material within a Gaussian accretion function centered at 1 AU^{-1} with FWHM of 0.60 AU^{-1}, its feeding zone stretched from 0.625 – 2.50 AU (i.e., inward of Venus at 0.723 AU to outward of Mars at 1.52 AU). The smaller width accretion functions simulate smaller feeding zones. The narrowest accretion functions studied correspond to a feeding zone of 0.94 – 1.06 AU for Earth. It is possible that Earth, Venus, and Mars had different size feeding zones and that the size of the feeding zones of each planet varied with time.

Barshay compared the zero pressure density; mean atomic weight, and volatile element mass fractions (for water, carbon, and sulfur) for the Earth and other terrestrial planets for different accretion functions of variable width. The zero pressure density is the uncompressed density of the mineralogy for each planet and the mean atomic weight in atomic mass units (amu) is the atom fraction weighted atomic weight of all metal – and rock – forming elements, e.g.,

$$\bar{\mu} = F_O\mu_O + F_{Si}\mu_{Si} + F_{Mg}\mu_{Mg} + F_{Fe}\mu_{Fe} + F_S\mu_S + F_{Al}\mu_{Al} + F_{Ca}\mu_{Ca} + \cdots$$

The general equation for computing the mean atomic weight is thus

$$\bar{\mu} = \sum_i F_i\mu_i$$

The index "i" represents an element and the summation is carried out for all elements in the calculations. For example, the mean atomic weight of the bulk Earth models in Table 2 are 25.2 (MF14), 25.9 (Kargel & Lewis 1993), 26.2 (McDonough 2003), and 26.3 (Morgan & Anders 1980). The BSE model of Palme & O'Neill (2014) has a mean atomic weight of 21.1 amu. Figure 5 shows calculated mean atomic weights of ~ 25.2 to ~ 25.7 for the widest to narrowest Gaussian accretion functions, respectively. These values fall within the range of mean atomic weights for our bulk Earth model (MF14) and Kargel & Lewis (1993). Higher mean atomic weights, like those from the McDonough (2003) and Morgan & Anders (1980) bulk Earth models, are produced in the square wave and triangular accretion function calculations in Figures 3 and 4.

For comparison the mean atomic weights (in amu) of some of the major chondrite groups are 15.0 (CI), 17.2 (CM), 22.4 (CV), 24.0 (CO), 24.7 (H), 23.3 (L), 22.7 (LL), and 25.9 (EH). The values for the EH and H chondrites are closest to those for the bulk Earth models in Table 2 and in Figures 3-5. The variations in the mean atomic weight of the different chondrite groups are related to their volatile (water, C, N) content (e.g., compare CI vs. CM, CV, CO chondrites) and Fe content (e.g., compare H, L, LL chondrites).

Another important conclusion from Barshay (1981) is that the chemical compositions (i.e., mean atomic weight) of the terrestrial planets Venus, Earth, and Mars are similar to one another because their accretion zones overlapped one another in the solar nebula. These results are consistent with prior ideas that the Earth formed from a mixture of nebular materials (e.g., the two component models of Ringwood and Wänke). It would be interesting to update his work using more sophisticated models of planetary accretion.

B-2. BSE and Bulk Earth composition

Similarity to chondritic meteorites (chondrites)

The overall composition of the BSE (in particular see Table 1 and Fig 2 in Palme & O'Neill 2014) and bulk Earth (e.g., Larimer 1971; Kargel & Lewis 1993) is close to chondritic, i.e., the relative proportions of the major rock-forming elements (Mg, Si, Fe, S, Al, Ca) are close to those found in chondritic meteorites (chondrites). Before discussing this point in more detail we present some background information about chondritic meteorites.

Chondrites are the most abundant kind of meteorites. They are unmelted stony meteorites that contain Fe-Ni metal alloy, silicate, sulfide, and oxide minerals in variable proportions. The chondrites are the oldest objects in the solar system with ages up to ~ 4.567 Ga (e.g. Amelin et al. 2002; Bouvier et al. 2007; Jacobsen et al. 2008). The relative abundance of rock-forming elements in chondrites is close to their relative abundances in the solar photosphere (e.g., Anders & Grevessse 1989; Lodders 2003; Palme et al. 2014; Suess & Urey 1956). Atmophile elements such as H, C, N, O, and noble gases are depleted relative to solar composition, and the light elements Li and B are enriched relative to solar composition (because they are destroyed by thermonuclear reactions in the Sun), but otherwise there is a close match between the composition of chondrites and that of the Sun. The five CI carbonaceous chondrites (Alais, Ivuna, Orgueil, Revelstoke, and Tonk), all of which are observed falls, are the closest in composition to the solar photosphere (Anders & Grevesse 1989; Lodders 2003; Palme et al. 2014).

The major different classes of chondrites, and the major groups within each class, are (1) carbonaceous chondrites (CI, CM, CO, CV, CK, CH, CB), comprising 3.1% by number of all chondrites, (2) ordinary chondrites (H, L, LL), which are 96.2% of all known chondrites, (3) enstatite chondrites (EH, EL), making up 0.6% of all chondrites, and (4) other chondritic classes (R, K) that are <0.1% of all chondrites (Krot et al. 2014). The different classes of chondrites are distinguished by different metal/silicate abundances, lithophile element ratios (e.g., Mg/Si, Al/Si, Na/Si), redox state, and oxygen isotopic (16, 17, 18) composition. All chondrites have been heated to varying extents and chondrite metamorphic grades are distinguished by various chemical and petrographic criteria such as presence or absence of glass, homogeneity of ferromagnesian silicates, abundance of volatile elements and presolar grains (McSween et al. 1988; Huss et al 2006).

As mentioned above, the chondrites are the most abundant kind of meteorites, and achondrites (melted stony meteorites), stony – iron meteorites, and iron meteorites are less abundant. As of the time of writing (June 2014), there are 44,332 known chondritic meteorites out of 47,520 meteorites of all kinds. Strictly speaking these statistics only give the abundance of meteoritic material in orbits that intersect the Earth and not the abundance of meteoritic material formed in the solar nebula and early solar system or existing in the asteroid belt today (e.g., Cloutis et al. 2014). We return to this question in the next section.

Chondritic material.

We emphasize that chondrites are not *pristine* samples of nebular material because the compositions of chondrites have been more or less altered by dry thermal metamorphism and/or aqueous alteration on their meteorite parent bodies (McSween et al. 1988; Huss et al. 2006). As discussed in the rest of this chapter we are interested in determining the type(s) of chondritic material that was (were) the building block(s) of the Earth. Following Schaefer & Fegley (2007, 2010) and Fegley & Schaefer (2014) we use the term "chondritic material" to refer to the pristine nebular material that formed chondrites. Thus carbonaceous chondritic material was the nebular precursor to carbonaceous chondrites, ordinary chondritic material was the nebular precursor to ordinary chondrites, and enstatite chondritic material was the nebular precursor to enstatite chondrites. Using this nomenclature, we do not have samples of chondritic material in our meteorite collections. Interplanetary dust particles (IDPs) are another analog to the chondritic material that existed in the solar nebula, but their bulk chemical and isotopic compositions are not as well known as that of meteorites. Perhaps in the future returned samples of relatively unaltered interior regions of comets will provide a closer approach to the original composition of some types of chondritic material. At the present time chondritic meteorites are the best samples that we have available; hence we use them in our discussion.

Preferred bulk Earth model

Table 2 gives our composition (MF14) for the bulk Earth based on BSE and core compositions given in the literature (e.g., Badro et al. 2014; Lodders & Fegley 1998, 2011; McDonough 2003; Palme & O'Neill 2014) and from arguments in this paper. It is calculated using equations analogous to the one for the bulk earth concentration of Mg, i.e., a weighted average of BSE and core concentrations of each element. Our bulk Earth composition uses the best-fit core composition of Badro et al. (2014), and solar Fe/Ni and Fe/Co ratios in the core. The bulk Earth oxygen abundance is identical to the arithmetic mean value for H-chondrites (within 1σ uncertainty), but the Mg/Si ratio is much higher than that for H-chondrites (0.82) and is identical to that for the more oxidized CO chondrites.

This may not be unexpected because Hart & Zindler (1986) emphasized that "the Earth is not like any chondrite (in major elements) but is composed of its own blend of accretion products, with a bias toward a higher proportion of the high temperature refractory components (or equivalently, a lower proportion of the volatiles and partially refractory components)."

Also, if Earth sampled material from a range of radial distances in the solar nebula, as physical accretion models predict (e.g., see the review by Chambers 2014), it will contain material of variable elemental composition. For example, the amount of oxidized Fe ($FeSiO_3$ in pyroxene, Fe_2SiO_4 in olivine, and magnetite) increases with decreasing temperature in the solar nebula (see Figures 1 and 2).

Badro et al. (2014) also found a core model containing 5.4% O, remainder Fe-Ni alloy also fit the seismic velocity and density data. In this case we compute a bulk

Earth model with ~ 35.3% O, 14.3% Si, 29.8% Fe, 1.68% Ni, and otherwise identical to that shown in Table 2. The oxygen abundance for this model is intermediate between the average values for H (33.86%) and L chondrites (36.93%), but the Mg/Si ratio of 1.05 is significantly higher than that of H (0.82) and L (0.80) chondrites or any of the major chondrite groups.

Chondritic vs. Achondritic Earth

Larimer (1971) considered whether the Earth is chondritic or achondritic (like eucrites) and concluded it is chondritic to first order. His arguments are worth revisiting because dating by three relative chronometers (^{182}Hf–^{182}W, ^{26}Al–^{26}Mg, and ^{53}Mn–^{53}Cr) indicates that the EHD (eucrite – howardite – diogenite, presumably from the asteroid 4-Vesta) meteorite parent body differentiated during the first 1–10 Ma of solar system history (e.g., Jacobsen et al., 2008; Schiller et al., 2011; Trinquier et al., 2008). The EHD meteorites are the major kind of achondrites (51% of all achondrites by number). Lead–lead (^{207}Pb–^{206}Pb), ^{26}Al–^{26}Mg, and ^{53}Mn–^{53}Cr dating also indicate that the parent body of the Asuka 881394 basaltic meteorite formed and differentiated within 3 Ma of solar system formation (Wadhwa et al., 2009). Consequently, Earth may have accreted a mixture of chondritic and achondritic material during its formation.

Table B-3 compares abundances of volatile lithophile elements in the bulk silicate Earth, average ordinary chondrites, and in the silicate portion of the eucrite parent body – here called bulk silicate Vesta BSV. (The bulk silicate Vesta models are described in the references cited.) Table B-3 shows that the bulk silicate Earth is depleted in volatile lithophiles relative to ordinary chondrites by factors of 0.04 (for

C and N) to 0.66 for F. Zinc, which behaves both as a lithophile and chalcophile, is not depleted relative to ordinary chondrites in the BSE. The large depletions for C and N in the BSE may also reflect their partial sequestration in the Earth's core as both elements occur in meteoritic metal and behave as siderophiles under some conditions. We do not give H contents for BSV because no reliable data are available. Sarafian et al. (2013, 2014) report analyses of OH-bearing apatite in eucrites but the H_2O content of the parental melts cannot be determined uniquely from apatite analyses (Boyce et al. 2014). The depletions for the alkalis (Na 0.37, K 0.30, Rb 0.29, Cs 0.30) are well known (e.g., Gast 1960; Hurley 1968; Larimer 1971) although the BSE data of Palme & O'Neill (2014) correspond to larger alkali abundances (i.e., smaller depletions) than estimated earlier. The explanations proposed for the observed alkali depletions in the BSE include (1) nebular fractionation of proto-Earth material, (2) evaporative loss during accretion, or (3) sequestration into Earth's core (e.g., see Palme & O'Neill 2014; Kargel & Lewis 1993; Lodders 2000). The first model implies that all elements with similar volatility will be equally fractionated. This is not the case because Zn is much less depleted in the BSE than Rb or Cs, which have similar 50% condensation temperatures (Lodders 2003). The second model requires loss of vapor from Earth's gravity field either by thermal escape or physical blow-off. The third model requires partitioning into Earth's core during its formation, and there is little experimental evidence for this (e.g., Corgne et al. 2007). Whatever the cause(s) for alkali depletion in the BSE may be, Table B-3 shows that volatile lithophile element depletions in bulk silicate Vesta are significantly larger than in the BSE. The volatile lithophile depletions on Vesta are presumably either inherited from the material accreted by Vesta or due to heating of Vesta. In any case, achondritic material like the EHD meteorites cannot supply the terrestrial abundances of carbon, nitrogen, halogens (Cl, Br), Zn, or alkalis (Na, K, Rb, Cs). Other types of achondrites are also depleted in volatile lithophiles relative to the BSE, e.g., angrites, mesosiderites, pallasites, and ureilites. The enstatite achondrites (aubrites) contain more volatile lithophiles than other achondrites and are an exception.

It is unlikely for at least two reasons that the Earth accreted *only* achondritic material during its formation. First, if the Earth did so, then its oxygen isotopic composition would be identical to that of achondritic material, e.g, the eucrites. This is not the case (e.g., see Figure 1 of Lodders & Fegley 1997). Second, chondritic material is significantly more abundant in our meteorite collections and in the asteroid belt than achondritic material (e.g., Cloutis et al. 2014). It would be difficult to believe that the Earth accreted *no* chondritic material. Instead it is more plausible that Earth accreted a mixture of achondritic and chondritic material. Third, the Earth has so many isotopic similarities to enstatite chondritic material that it seems likely that enstatite chondrites and the Earth are somehow related to one another. This could not happen if the Earth formed solely from achondritic material. For example, oxygen isotope mixing models (Lodders 1991, 2000; Lodders & Fegley 1997) predict that E-chondritic material is an important building block of the Earth, Mars, and 4-Vesta.

It is possible that accretion of volatile – poor achondritic material could be balanced by accretion of more volatile – rich chondritic material. In principle the relative mass fractions of achondritic and chondritic components can be constrained by an oxygen isotopic mixing model (e.g., Lodders 1991, 2000; Lodders & Fegley 1997), but this is beyond the scope of this review chapter because the abundances of all natural elements – not only volatile lithophiles – need to be considered simultaneously in the modeling.

Isotopic arguments:

Until the early 1970s, it was assumed that the hot solar nebula was chemically and isotopically homogeneous; however, the discoveries of isotopic anomalies in refractory inclusions of meteorites, which cannot be explained by radioactive decay, cosmogenic effects or mass fractionations, have lead to revisions of this concept (Clayton et al. 1973). Planetary processing such as core formation or magmatic differentiation can only produce mass-dependent isotopic fractionations and therefore do not modify isotopic anomalies, so terrestrial surface samples can be considered isotopically representative of the bulk Earth for comparison with meteoritic materials.

Following the discovery of oxygen isotopic variations among meteorites and planetary materials, isotopic variability has been found for other elements, and combining these different isotopic systems is one of the best tracers to determine the Earth's building blocks.

Isotopic variability between solar system materials can be accounted for by few mechanisms:

-Stable isotope fractionations, which originate from vibrational energy partitioning between coexisting phases at equilibrium or under kinetic conditions (e.g.

Bigeleisen & Mayer 1947). At first order, this process is proportional to the mass-difference between the isotopes; however, non-mass dependent effects have been observed in some systems (e.g. Thiemens 1999; Moynier et al. 2013).

-Nuclear reactions such as the decay of long-lived (e.g. ^{87}Rb-^{87}Rb) or short-lived (e.g. ^{26}Al-^{26}Mg) radioactive isotopes or spallation by cosmic rays or solar wind.

-Inheritance of isotopic heterogeneities, which originated from an incomplete mixing of nucleosynthetic products. These effects are observed after correction of isotopic ratios for stable isotope fractionation, radioactive decay, and spallation effects.

To identify which group(s) of meteorites (if any) represents the composition of the Earth, nucleosynthetic anomalies, radiogenic isotopes produced by short-lived radioactivity (e.g. ^{142}Nd) and stable isotope fractionations (e.g. Si isotopes) can be used. In the following section we will present these different arguments.

Applications of isotopic anomalies

Since isotopic anomalies cannot be modified by planetary differentiation they are usually considered to be very robust tracers of the Earth's building blocks. Among the different meteorite groups, the Enstatite (E) chondrites are the closest to the terrestrial mantle in term of isotopic composition (See Figure 6). Isotopic anomalies are either reported as the deviation from the mass-fractionation line in a three-isotope diagram (the so-called Δ notation (e.g. Δ^{17}O)) or using the ε–notation which represents the per ten thousand deviation of an isotopic ratio normalized to another isotopic ratio of the same element. Therefore, isotopic anomalies can only be investigated for elements with at least three isotopes.

Elements for which isotopic anomalies have been found in one or more groups of meteorites are: oxygen (e.g. Clayton 1993), titanium (Trinquier et al. 2009; Zhang et al. 2012), calcium (Simon et al. 2009; Moynier et al. 2010), chromium (e.g. Trinquier et al. 2007; Qin et al. 2010), nickel (e.g. Regelous et al. 2008; Steele et al.2012), strontium (Moynier et al. 2012), zirconium (Akram et al. 2013), molybdenum (e.g. Dauphas et al. 2002; Yin et al. 2002; Burkhardt et al. 2011), ruthenium (Chen et al. 2010), barium (Carlson et al. 2007, Andreasen and Sharma 2007, Ranen et al. 2007), neodymium (Carlson et al. 2007) and samarium (Andreasen and Sharma 2007). The elements for which all solar system materials have similar isotopic composition within error are: zinc (Moynier et al. 2009), iron (Wang et al. 2011; Tang and Dauphas 2012), tellurium (Fehr et al. GCA 2006), osmium (Yokoyama et al. 2007), silicon (Pringle et al. 2013), and hafnium (Sprung et al. 2010). The absence of isotopic anomalies for some elements but presence of anomalies for others is not completely understood; to date the best explanation suggests a decoupling between the phases carrying the elements with anomalies and those without, which are homogenized to different degrees.

Most elements show a similar isotopic composition between the Earth (estimated by measurements of mantle rocks) and enstatite chondrites (EH and EL) (see figure 6). This isotopic coincidence has been used to propose a strong genetic link between the Earth and enstatite chondrites, and in some cases to use enstatite chondrites as the main building blocks for the Earth (Javoy et al. 1995; Javoy et al.

2010; Jacobsen et al. 2012). The main problem with making the Earth from enstatite chondrites comes when considering the chemical composition (see above); among other dissimilarities, they have insufficient FeO, low Mg/Si ratio, and overabundant volatile elements. In order to reconcile the chemistry of enstatite chondrites with what we know of the terrestrial mantle, Javoy et al. (2010) proposed that enstatite chondrites were devolatilized prior to accreting to form the Earth (to account for the depletion of the Earth in volatile elements) and that the Earth is chemically heterogeneous and the remainder of the chemical differences are stored in the lower mantle. Alternatively, Jacobsen et al. (2012) proposed that the material that formed the Earth and the E-chondrites had a common nebular precursor, but a secondary event modified the chemical composition of the enstatite chondrites without altering the isotopic composition.

It must be noted that three recent studies have shown that the terrestrial isotopic composition of Mo (Burkhardt et al. 2011), Ti (Zhang et al. 2012) and O (Herwartz et al. 2014) do not exactly match E-chondrites and the Earth. While Zhang et al. (2012) do not discuss this possible difference in Ti isotopes between E-chondrites and the Earth, Burkhardt et al. (2011) propose that no known type of chondrites are representative of the bulk Earth for Mo isotopes. However, when the analytical errors are taken into account (see Figure 6) EH are similar to Earth for both Ti and Mo isotopes, while EL are slightly different. In addition, only one EH and one EL have been analyzed for Mo isotopic composition, and more data are needed to resolve this issue.

On the other hand, the recent high precision oxygen isotopes of Herwartz et al. 2014 show a clear $\Delta^{17}O$ difference between the Earth, the Moon (12ppm heavier than Earth) and the E-chondrites (60 ppm heavier than Earth). This represent a major observation which suggests that the Earth cannot be formed from E-chondrites alone as developed above based on major element composition and as we will developed below based on isotope ratio.

Another line of interpretation of the isotopic anomalies is that the Earth represents a mixing between different types of chondrites (Lodders 2000, Warren et al. 2011). Lodders (2000) used O isotopic compositions to calculate the best mixing model in order to account for the composition of the Earth and obtained 70% EH, 21% H, 5% CV, and 4% CI. Following the same logic, Fitoussi and Bourdon (2012) expanded this work by combining multiple isotopic systems (O, Cr, and Ni isotopes). They found that a good mixing relation would involve 63% LL, 16% CI and 23% CO.

Mixing different types of chondrites can clearly reproduce the isotopic composition of the Earth, the very close proximity between E-chondrites and the Earth suggest that these meteorites may have close connection to the Earth in terms of their isotopic composition but does not simply prove that the Earth has been made of E-chondrite materials.

Radiogenic isotopes

The discovery of a 20ppm excess of the $^{142}Nd/^{144}Nd$ in terrestrial rocks compared to any chondrite group had fundamental consequences on our understanding of the Earth's mantle (Boyet and Carlson 2005). ^{142}Nd is produced by the radioactive decay of ^{146}Sm (half life of 103 Ma). This is a short-lived radioactive system that can only record Sm/Nd fractionation that occurred during the first 500Ma of Earth's history. This terrestrial excess in ^{142}Nd has been interpreted as the result of the decay of ^{146}Sm in a suprachondritic Sm/Nd reservoir, which formed by partial melting of the Earth's primitive mantle and is referred to as the early-depleted reservoir (see Carlson et al. this volume). Its counterpart, the early enriched reservoir, with a low Sm/Nd ratio and a depletion in ^{142}Nd (compared to chondrites), would have been either incorporated within the Earth's mantle and not recorded in geological samples (a hidden reservoir, Boyet and Carlson 2005) or lost to space following an asteroid impact (impact erosion, e.g. O'Neill and Palme 2008; Caro and Bourdon 2010). A hidden reservoir would mean that the Earth's mantle has a chondritic composition for the refractory lithophile elements, whereas an impact erosion loss of an early-enriched reservoir would imply that the bulk silicate Earth does not have a chondritic abundance of lithophile elements.

Stable isotope fractionation

Stable mass-dependent isotopic variations between meteorites and planetary bodies are attributable to processes that fractionated isotopes during nebular events (e.g. Luck et al. 2003) or during planetary events such as core formation (e.g. Georg et al., 2007; Moynier et al., 2011). Among the major elements, only O, Si, and Ca show mass-dependent isotopic fractionation between different chondrite groups and can potentially be used as tracers of the Earth's building blocks (e.g. Clayton et al. 1993; Fitoussi et al. 2011; Valdes et al. 2014). Other multi-isotopic major elements such as Mg (e.g. Teng et al. 2007) and Fe (e.g. Poitrasson et al. 2004) do not show any mass-dependent isotopic variations between chondrite groups and therefore are not useful to investigate the Earth's building blocks and will not be discussed here.

A small heavy Si isotopic enrichment in Bulk Silicate Earth (BSE) compared to chondrites has been interpreted as evidence for the incorporation of ~4-7 wt.% silicon as a light element into the Earth's core (Georg et al., 2007; Fitoussi et al., 2009; Savage and Moynier 2013; Armytage et al., 2011). Fitoussi and Bourdon (2012) used the observation that enstatite chondrites are significantly lighter than Earth in Si isotope compositions to argue that the BSE cannot consist of more than 15% of enstatite chondrite precursor material. Their logic was that since the BSE has a $^{30}Si/^{28}Si$ ratio ~0.30 permil heavier than the E-chondrites, unrealistically large amounts of Si (>20 wt.%) would need to have entered the Earth's core if the bulk Earth had E-chondritic Si isotope compositions; therefore, the density constraints placed on the amount of light elements in the Earth's core coupled with the fact that E-chondrites are Si-rich significantly limits the amount of E-chondritic material as building blocks of Earth. On the other hand, Savage and Moynier (2013) have shown that the light Si isotopic composition of the E-chondrites is carried by the metal phases, and enstatite minerals have a similar Si isotopic composition to the carbonaceous chondrites. They argued that E-chondrites could not be the building blocks of the Earth, but materials enriched in refractory siderophile elements that condensed in the same region as the E-chondrites could be a major component of the Earth.

Calcium isotopes are potentially very useful tracers of the Earth's building blocks, but until recently there were no high precision Ca isotope data available (Simon and DePaolo 2011, showed that different chondrite groups have unique stable Ca isotopic compositions (see Figure 7): the carbonaceous chondrites are isotopically lighter and the E-chondrites are heavier than BSE. On the other hand, the ordinary chondrites were isotopically similar to BSE. This led Simon and Depaolo to exclude E-chondrites and C-chondrites as representative building blocks for the Earth. However, a more recent study has shown that although most C-chondrite groups are isotopically lighter than the Earth, the CO chondrites are similar to Earth in Ca isotopes (Valdes et al. 2014, see figure 7). In addition, this new study has shown that the E-chondrites are similar to the Earth, and therefore it is not possible to exclude the E- chondrites as building blocks of Earth based on Ca isotopes (Valdes et al. 20014; Huang et al. 2012).

In conclusion, stable isotopes are not as powerful tracers for the Earth's building block as nucleosynthetic anomalies since their abundances can be modified by planetary processes. However, it seems clear that based on Si isotopes, it is improbable to form the Earth from pure E-chondrites since this would require amounts of Si in the core in excess of 20 wt.%. It should be noted that a recent theoretical study (Huang et al. 2014), has shown that Si isotopes might be fractionated within the mantle. Due to the large difference in pressure within the Earth's mantle, high-pressure minerals containing Si (e.g. perovskite-structured silicate) have a different structure than those at lower pressure (e.g. olivine or ringwoodite). This phenomenon is known as a phase transition and results in a change in atomic bonding, or coordination; the calculations of Huang et al. (2014) indicate that Si isotopes may be fractionated between silicate minerals with different coordinations of Si. If these results are correct, they could have important implications for the composition of the core and the conditions of formation of the Earth. Specifically, even a small fractionation of Si isotopes in the mantle could drastically decrease the need for large quantities of Si in the Earth's core to account for the difference between the measurable upper mantle and chondrites in Si isotope composition. This would change the conclusions regarding the building blocks of the Earth based on the Si isotopes. Since these isotopic fractionation results are only theoretical, this effect must be tested experimentally before strong conclusions can be made. In addition, Pringle et al. (2014) have found that angrite meteorites, which are highly oxidized achondrites, have the same Si isotopic composition as the Earth and therefore different from chondrites. Since these meteorites are oxidized it is very unlikely that the core of the angrite parent body is very rich in Si. These results suggest that other mechanisms of isotopic fractionation (e.g. volatilization) may fractionate Si isotopes in the early solar system, and that Si isotopes might not be such a strong argument to exclude enstatite chondrites from the Earth's building blocks.

Conclusions

In this review paper we propose a new estimate for the bulk chemical composition of the Earth by combining seismological observations, chemical analyses of the atmosphere, biosphere, hydrosphere, crust, and mantle, experimental results of elemental partitioning, ratios of elements with very similar geochemical behavior and recent theoretical estimates of the core composition by molecular dynamics simulations of density and sound speed (Table 2). High-precision isotopic studies are fundamental in establishing compositional relationships between meteorites and the Earth. We show that non-mass-dependent isotopic variations, which are not modified by planetary processes, are the best tracers to search for the genetic origin of the Earth since crustal rocks can be directly compared to meteorites. Enstatite chondrites are the meteorites isotopically closest to Earth. However, they are chemically very different from the estimate of the bulk Earth composition (See Table 2), which suggests that either (1) the Earth is not made of any known meteorites or from the mixing of different groups of meteorites in proportions that would fit the isotopic composition of the Earth or (2) the Earth and enstatite chondrites share a common ancestor but their chemical evolution diverged early in the Solar System history.

Acknowledgments. B.F. was supported by the NASA EPSCOR Program and by NASA Cooperative Agreement NNX09AG69A with the NASA Ames Research Center. FM thanks the ANR for a chaire d’Excellence Sorbonne Paris Cité, for the UnivEarthS Labex program (ANR-10-LABX-0023 and ANR-11-IDEX-0005-02) and the INSU for a PNP grant. We thank K. Lodders, M. Moreira, P. Savage and E. Pringle for discussions and the referees for their comments, which led to some of our stronger and more clear statements.

References

Allègre, C.J., Poirier, J.P., Humler, E., and Hofmann, A.W. (1995) The chemical composition of the Earth. Earth Planet. Sci. Lett. 134, 515-526.

Allègre, C.J., Hofmann, A., O'Nions, K. (1996) The argon constraints on the mantle structure. Geophys. Res. Lett. 23, 3555-3557.

Albarede, F. (1998) Time-dependent models of U-Th-He and K-Ar evolution and the layering of mantle convection. Chem. Geol. 145, 413-429.

Anderson, D. L. (2002) The case for irreversible chemical stratification of the mantle. Intl. Geol. Rev. 44, 97-116.

Andreasen and Sharma (2007) Mixing and homogenization in the early solar system: clues from Sr, Ba, Sm,and Nd isotopes in meteorites. Astrophys. J. 665, 874-883.

Akram, W. Schonbachler, M., Sprung, P., Vogel, N. (2013) Zircon-hafnium isotope evidence from meteorites for the decoupled synthesis of light and heavy neutron-rich nuclides. Astrophys. J. 777, 169

Amelin, Y., Krot, AN, Hutcheon, IA, Ulianov, AA. (2002) Lead isotopic ages of chondriles and Calcium Aluminium Rich inclusions. Science. 297, 1678-1683

Armytage, R. M. G., Jephcoat, A. G., Bouhifd, M. A., and Porcelli, D. (2013) Metal – silicate partitioning of iodine at high pressures and temperatures: Implications for the Earth's core and ^{129*}Xe budgets. Earth Planet. Sci. Lett. 373, 140-149.

Armytage, R.M.G., Georg, R.B., Savage, P.S., Williams, H.N., Halliday, A.N. (2011) Silicon isotopes in meteorites and planetary core formation. Geochim. Cosmochim. Acta. 75, 3662-3675

Badro, J., Côté, A. S., and Brodholt, J. P. (2014) A sesimologically consistent compositional model of Earth's core. Proc Natl. Acad Sci USA doi/10.1073/pnas.1316708111.

Ballentine, C. J. and Holland, G. (2008) What CO_2 well gases tell us about the origin of noble gases in the mantle and their relationship to the atmosphere. Phil. Trans. Royal Soc. of London 366A: 4183–4203.

Barshay, S. S. (1981) Combined Condensation – Accretion Models of the Terrestrial Planets. PhD Thesis, MIT, Cambridge, MA.

Bigeleisen, J. and Mayer, M.G. (1947) Calcualtion of equilibrium constants for or isotopic exchange reactions. J. Chem. Phys. 15. 261-267

Bina, C. R., and Helffrich, G. (2014) Geophysical constraints on mantle composition. Chapter 3.2 in Treatise on Geochemistry, 2nd ed., Elsevier.

Birch, F. (1952) Elasticity and constitution of the Earth's interior. J. Geophys. Res. 57, 227-286.

Birch, F. (1964) Density and composition of mantle and core. J. Geophys. Res. 69, 4377-4388.

Bouhifd, M. A., Jephcoat, A. P., Heber, V. S., and Kelley, S. P. (2013) Helium in Earth's early core. Nature Geosci. 6, 982-986.

Bouhifd, M. A., Andrault, D., Bolfan-Casanova, N., Hammouda, T., and Devidal, J. L. (2013) Metal – silicate partitioning of Pb and U: Effects of metal composition and oxygen fugacity. Geochim. Cosmochim. Acta 114, 13-28.

Bouvier A., Blichert-Toft J., Moynier F., Vervoort J. and Albarède F. (2007) New Pb-Pb ages relevant to the accretion and cooling history of chondrites. Geochimica et Cosmochimica Acta 71, 1583-1604

Boyce, J.W., Tomlinson, S.M., McCubbin, F.M., Greenwood, J.P., Treiman, A.H. (2014) The lunar apatite paradox. Science. 344, 400-402.

Boyet, M. and Carlson, R. (2005) 142^{Nd} evidence for early (>4.53Ga) global differentiation of the silicate Earth. Science. 309, 575

Brock, D. S. and Schrobilgen, G. J. (2011) Synthesis of the missing oxide of xenon, XeO_2, and its implications for Earth's missing xenon. J. Am. Chem. Soc. 133: 6265–6269.

Burkhardt, C., T. Kleine, F. Oberli, A. Pack, B. Bourdon, R. Wieler (2011), Molybdenum isotope anomalies in meteorites: Constraints on solar nebula evolution and origin of the Earth, Earth Planet. Sci. Lett. 312, 390-400.

Cameron, A.G.W. (1995) The first ten million years in the solar nebula. Meteoritics 30, 133-161.

Cameron, A.G.W., Fegley, B., Jr., Benz, W., & Slattery, W.L. (1988) The Strange Density of Mercury: Theoretical Considerations, in *Mercury*, eds. M.S. Matthews, C. Chapman & F. Vilas, pp. 692-708, Univ. of Arizona Press, Tucson, AZ.

Carlson, R., W., Boyet, M., Horan, M. (2007) Chondrite barium, neodymium and samarium isotopic heterogeneity and early Earth differentiation. Science 316, 1175

Carlson, R.W., Garnero, E., Harrison, T.M., Li, J., Manga, M., McDonough, W.F., Mukhopadhyay, S., Romanowicz, B., Rubie, D., Williams, Q., and Zhong, S. (2014) How did early Earth become our modern world? Annu. Rev. Earth Planet. Sci., in press.

Caro, G. and Bourdon, B. (2010) Non-chondritic Sm/Nd ratio in the terrestrial planets: Consequences for the geochemical evolution of the mantle-crust system. Geochim. Cosmochim. Acta. 74, 3333-3349.

Chambers, J.E. (2014) Planet formation. Chapter 2.4 in Treatise on Geochemistry 2nd ed. Elsevier.

Chen, J., Papanastassiou, D., Wasserburg, G.J. (2010) Ruthenium endemic isotope effects in chondrites and differentiated meteorites. Geochim. Cosmochim. Acta. 74, 3851-3862

Clayton, R. N. L., Grossman, L., Mayeda, T.K. (1973) A component of primitive nuclear composition in carbonaceous chondrites, Science, 182, 485-488.

Clayton R. N. (1993) Oxygen isotopes in meteorites. Ann. Rev. Earth. Planet. Sci. 21, 115–149.

Clayton, R.N. and Mayeda, T.K. (1996) Oxygen isotope studies in achondrites. Geochim. Cosmochim. Acta. 60, 1999-2017.

Clayton, R.N. and Mayeda, T.K. (1999) Oxygen isotope studies of Carbonaceous chondrites. Geochim. Cosmochim. Acta. 63, 2089-2104.

Clayton, R.N., Mayeda, T.K., Goswami, J.N., Olsen, E.J. (1991) Oxygen isotope studies of ordinary chondrites. Geochim. Cosmochim. Acta. 55, 2317-2337.

Cloutis, E. A., Binzel, R. P., and Gaffey, M. J. (2014) Establishing asteroid – meteorite links. Elements 10, 25-30.

Corgne, A., Keshav, S., Fei, Y., and McDonough, W. F. (2007) How much potassium is in Earth's core? New insights from partitioning experiments. Earth Planet. Sci. Lett. 256, 567-576.

Dauphas, N., Marty, B., & Reisberg, L. (2002) Molybdenum evidence for inherited planetary scale isotope heterogeneity of the protosolar nebula. Astrophys. J. 565, 640-644.

Dauphas, N. and Morbidelli, A. (2014) Geochemical and planetary dynamical views on the origin of Earth's atmosphere and oceans. Chapter 6.1 in Treatise on Geochemistry 2nd ed. Elsevier.

DeCampli, W. M. and Cameron, A. G. W. (1979) Structure and evolution of isolated giant gaseous protoplanets. Icarus 38, 367-391.

Dreibus, G., and Wänke, H. (1980) The bulk composition of the eucrite parent asteroid and its bearing on planetary evolution. Z. Naturf. 34a, 204-216.

Dreibus, G., Brückner, J., and Wänke, H. (1997) On the core mass of asteroid Vesta. Meteoritics Planet. Sci. 32, A36.

Fegley, B., Jr. and Schaefer, L. K. (2014) Chemistry of Earth's earliest atmosphere. Chapter 6.3 In Treatise on Geochemistry 2nd ed. Elsevier.

Fehr, M., Rekhamper, M., Halliday, A.N., Wiechter, U., Hattendorf, B., Gunther, D., Ono, S., Eigenbrode, J., Rumble, D, III. (2005) Tellurium isotopic composition of the early solar system-A search for effect resulting from stellar nucleosynthesis, ^{126}Sn decay, and mass-independent fractionation. Geochim. Cosmochim. Acta, 69, 5099-5112.

Fitoussi, C., and Bourdon, B. (2012) Silicon isotope evidence against an enstatite chondrites Earth. Science. 335, 1477-1480.

Gast, P. W. (1960) Limitations on the composition of the upper mantle. J. Geophys. Res. 65, 1287-1297.

Genda, H. and Abe, Y. (2003a) Survival of a proto-atmosphere through the stage of giant impacts: The mechanical aspects. Icarus 164: 149–162.

Genda, H. and Abe, Y. (2003b) Modification of a proto-lunar disk by hydrodynamic escape of silicate vapor. Earth Planets Space 55, 53-57.

Genda H and Abe Y (2005) Enhanced atmospheric loss on protoplanets at the giant impact phase in the presence of oceans. Nature 433: 842–844.

Grossman, L. and Larimer, J. W. (1974) Early chemical history of the solar system. Rev. Geophys. Space Phys. 12, 71-101.

Hart SR and Zindler A (1986) In search of a bulk-earth composition. Chemical Geology 57: 247–267.

Helffrich, G. R., and Wood, B. J. (2001) The Earth's mantle. Nature 412, 501-507.

Henning, T., and Semenov, D. (2013) Chemistry in protoplanetary disks. Chem. Rev. 113, 9016-9042.

Herwatz, D., Pack, A., Friedrich, B., Bischoff, A. (2014) Indentification of the giant impactor Theia in lunar rocks. Science. 344, 1146-1150.

Hirschmann, M. M., and Dasgupta, R. (2009) The H/C ratios of Earth's near-surface and deep reservoirs, and consequences for deep Earth volatile cycles. Chem. Geol. 262, 4–16.

Huang, S. and Jacobsen, S.B. (2012) Calcium isotopic variations in chondrites: implications for planetary isotope compositions. *Lunar Planet. Sci. Conf. 43,* #1334 (abstr.).

Huang, S., Farkas, J, Jacobsen, S. (2011) Stable calcium isotopic composition of Hawaiian shield lavas: Evidence for recycling of ancient marine carbonates into the mantle. Geochim. Cosmochim. Acta. 75, 4987-4997.

Huang, F., Wu, Z., Huang, S., Wu, F. (in press) First Calculations of equilibrium silicon isotope fractionation among mantle minerals, Geochim. Cosmochim. Acta.

Huang, S., Jacobsen, S.B., and Mukhopadhyay, S. (2013) ^{147}Sm – ^{143}Nd systematics of Earth are inconsistent with a superchondritic Sm/Nd ratio. PNAS 110(13), 4929-4934.

Hurley, P. M. (1968) Absolute abundance and distribution of Rb, K, and Sr in the Earth. Geochim. Cosmochim. Acta 32, 273-283.

Huss, G. R., Rubin, A. E., and Grossman, J. N. (2006) Thermal metamorphism in chondrites. In Meteorites and the Early Solar System II, (Eds. D. S. Lauretta, H. Y. McSween, and R. P. Binzel), pp. 567-586, University of Arizona Press, Tucson.

Jacobsen S. B., Ranen M. C., Petaev M. I., Remo J. L. , O'Connell R. J., and Sasselov D. D. (2008) Isotopes as clues to the origin and earliest differentiation history of the Earth. Phil. Trans. Royal Soc. of London 366A, 4129–4162.

Jacobsen, S.B., Petaev, M.I., Huang, S., Sasselov, D.D. (2013) An isotopically homogeneous region of the inner terrestrial planet region (Mercury to Earth) : Evidence from E chondrites and implications for giant-Moon impact forming scenario. Lunar and Planetary Sci. Conf. 44, #2344.

Jagoutz, E., Palme, H., Baddenhausen, H., Blum, K., Cendales, M., Dreibus, G., Spettel, B., Lorenz, V., and Wänke, H. (1979) The abundances of major, minor, and trace elements in the earth's mantle as derived from primitive ultramafic nodules. Proc. Lunar Planet. Sci. Conf. 10th, 2031-2050.

Javoy M. (1995) The integral enstatite chondrites model of the Earth. Geophys. Res. Lett. 22, 2219-2222.

Javoy, M., Kaminski, E., Guyot, F., Andrault, D., Sanloup, C., Moreira, M., Labrosse, S., Jambon, A., Agrinier, P., DAvaille, A., Jaupart, C. (2010) The chemical composition of the Earth: enstatite chondrite models. Earth Planet. Sci. Lett. 293, 259-268.

Javoy, M., Balan, E., MEheut, M., Blanchard, M., Lazzeri, M. (2012) First principles investigation of equilibrium isotopic fractionation of O and Si isotopes between refractory solids and gases in the solar nebula. Earth Planet. Sci. Lett. 319-320, 118-127.

Kargel, J. S., and Lewis, J. S. (1993) The composition and early evolution of the Earth. Icarus 105, 1-25.

Krot, A. N., Keil, K., Scott, E. R. D., Goodrich, C. A., and Weisberg, M. K. (2014) Classification of meteorites and their genetic relationships. Chapter 1.1 in Treatise on Geochemistry 2nd ed. Elsevier.

Larimer, J. W. (1967) Chemical fractionations in meteorites, 1. Condensation of the elements. Geochim. Cosmochim. Acta 31, 1215-1238.

Larimer, J. W. (1971) Composition of the Earth: Chondritic or achondritic. Geochim. Cosmochim. Acta 35, 769-786.

Lewis, J. S. (1972) Metal/silicate fractionation in the solar system. Earth Planet. Sci. Lett. 15, 286-290.

Lewis, J. S. (1974) The temperature gradient in the solar nebula. Science 186, 440-443.

Lewis, J. S. and Prinn, R. G. (1984) Planets and their atmospheres: Origin and evolution. Academic Press, NY.

Lodders, K. (1991) *Spurenelementverteilung zwischen Sulfid und Sili- katschmelze und kosmochemische Anwendungen.* Ph.D. thesis, Univ. Mainz, Germany

Lodders, K. (2000) An oxygen isotope mixing model for the accretion and composition of rocky planets. Space Sci. Rev. 92, 341-354.

Lodders, K. (2003) Solar system abundances and condensation temperatures of the elements. Astrophys. J., 591, 1220-1247.

Lodders, K. and Fegley, B., Jr. (1997) An oxygen isotope model for the composition of Mars. Icarus 126, 373-394.

Lodders, K. and Fegley, B. Jr. (1998) *The Planetary Scientist's Companion*. New York: Oxford University Press.

Lodders, K. and Fegley B., Jr. (2011) *Chemistry of the Solar System*. Cambridge: RSC Publishing.

Luck, J.M., Ben Othman, D., Barrat, J.A., Albarede, F. (2003) Coupled ^{63}Cu and ^{16}O excesses in chondrites. Geochim. Cosmochim. Acta, 67, 143-151

Lupu, R.E., Zahnle, K., Marley, M.S., Schaefer, L., Fegley, B., Morley, C., Cahoy, K., Freedman, R., and Fortney, J.J. (2014) The atmospheres of Earthlike planets after giant impact events. Astrophys. J., 784:27 doi:10.1088/0004-637X/784/1/27

Lyons, J.R., and Young, E.D. (2005) CO self-shielding as the origin of oxygen isotopic anomalies in the early solar nebula. Nature 435, 317-320.

Marty, B. (2012). The origins and concentrations of water, carbon, nitrogen and noble gas on Earth. Earth Planet. Sci. Lett. *313-314*, 56–66.

McDonough, W. F. (2003) Compositional models for the Earth's core. In: Carlson RW (ed.) Treatise on Geochemistry, Vol. 2, The Mantle and Core, pp. 547–568. Oxford: Elsevier-Pergamon.

McDonough, W. F., and Sun, S.S. (1995) The composition of the Earth. Chem. Geol. 120, 223-253.

McSween Jr., H.Y., Sears, D.W.G., Dodd, R.T., 1988. Thermal metamorphism. In: Kerridge, J.F., Matthews, M.S. (Eds.), Meteorites and the Early Solar System. University of Arizona Press, Tucson, pp. 102–113.

Morgan, J. W. and Anders, E. (1980) Chemical composition of Earth, Venus, and Mercury. Proc Natl. Acad Sci USA 77, 6973-6977.

Moynier, F., Dauphas, N., Podosek, F.A. (2009) A search for ^{70}Zn anomalies in meteorites. Astrophys. J., 700, L92-L95

Moynier, F., Simon, J.I., Podosek, F.A., Meyer, B.S., Brannon, J., DePaolo, D. (2010) Ca isotope effect in Orgueil leachates and the implications for the carrier phases of ^{54}Cr anomalies. Astrophys. J. Lett. 719, L7-L13.

Moynier, F., Yin, Q-z, Schauble, E. (2011) Isotopic evidence for Cr partitioning into the Earth core. Science, 331, 1417-1420.

Moynier, F., Day, J. Okui, W., Yokoyama, T., Bouvier, A., Walker, R.J., Podosek, F.A. (2012) Planetary scale Sr isotopic heterogeneity and the age of volatile depletion of the Early solar system materials. Astrophys. J. 758, 45-51.

Moynier, F., Fujii, T., Brennecka, G.A., Nielsen, S. (2013) Nuclear field shift in natural environments. Comptes Rendus Geoscience 345, 150-159.

Nishio-Hamane, D., Yagi, T., Sata, N., Fujita, T., and Okada, T. (2010) No reactions observed in Xe–Fe system even at Earth core pressures. Geophys. Res. Lett. 37: L04302.

O'Neill, H. St. C and Palme, H. (2008) Collisional erosion and the non-chondritic composition of the terrestrial planets. Phil. Trans. R. Soc. 366, 4205-4233

Ozima, M. and Podosek, F. A. (2001) Noble Gas Geochemistry, 2nd ed. Cambridge University Press.

Pahlevan, K. (2010) Chemical and isotopic consequences of lunar formation via giant impact. Ph.D. thesis, Caltech, Pasadena, CA.

Palme, H., and Nickel, K.G. (1985) Ca/Al ratio and the composition of the Earth's upper mantle. Geochim. Cosmochim. Acta 49, 2123-2132.

Palme, H., and O'Neill, H. St. C. (2014) Cosmochemical estimates of mantle composition. Chapter 3.1 in Treatise on Geochemistry, 2nd ed., Elsevier.

Pepin, R. (2006) Atmospheres on the terrestrial planets: Clues to origin and evolution. Earth Planet. Sci. Lett. 252, 1-14

Perryman, M. (2011) The Exoplanet Handbook. Cambridge University Press.

Poitrasson, F., Halliday, AN., Lee, D.C., Levasseur, S., Teush, N. (2004) Iron isotope differences between Earth, Moon, Mars, and Vesta of possible records of contrasted accretion mechanisms. Earth Planet. Sci. Lett. 223, 253-266.

Prinn, R. G. and Fegley, B., Jr. (1989) Solar nebula chemistry: Origin of planetary, satellite, and cometary volatiles. In *Origin and Evolution of Planetary and Satellite Atmospheres,* eds. S. Atreya, J. Pollack & M.S. Matthews, pp. 78-136, Univ. of Arizona Press, Tucson, AZ.

Pringle, E., Savage, P., Jackson, M.G., Barrat, J.A., Moynier, F. (2013) Si isotope homogeneity of the Solar Nebula. Astrophys. J. 779, 123.

Pringle, E.A., Savage, P., Badro, J., Barrat, J.A., Moynier F. (2014) Silicon isotopes in achondrites and clues to planetary differentiation. Goldschmidt conference abstract.

Pujol, M., Marty, B., Burgess, R. (2011) Chondritic-like xenon trapped in Archean rocks: A possible signature of the ancient atmosphere. Earth Planet. Lett. 208, 398-406.

Qin, L., Alexander, CMOD, Carlson, R.W., Horan, M.F., Yokoyama, T. (2010) Contributors to chromium isotope variations in meteorites. Geochim. Cosmochim. Acta. 74, 1122-1145.

Ranen, M., and Jacobsen, S. (2007) Barium isotopes in chondritic meteorites: implications for planetary reservoirs models. Science. 314, 809-812.

Regelous, M., Elliott, T., Coath, C.D. (2008) Nickel isotope heterogeneity in the early solar system, Earth Planet. Lett. 372, 330-338.

Ringwood, A.E. (1979) Origin of the Earth and Moon. Springer-Verlag, Berlin.

Saal, A. E., Hauri, E. H., Langmuir, C. H., and Perfit, M. R. (2002) Vapour undersaturation in primitive mid-ocean-ridge basalt and the volatile content of Earth's upper mantle. Nature 419: 451–455.

Sanloup, C. Schmidt, B. C., Chamorro Perez, E. M., et al. (2005) Retention of xenon in quartz and Earth's missing xenon. Science 310: 1174–1177.

Sanloup,. C, Schmidt, B.C., Gudfinnsson, G., Dewaele, A., and Mezouar, M. (2011) Xenon and argon: A contrasting behavior in olivine at depth. Geochim. Cosmochim. Acta 75, 6271–6284.

Sarafian, A.R., Roden, M.F., Patino-Douce, A. (2013) The volatile content of Vesta: clues from apatite in eucrites. Met. & Planet. Sci. 48, 2135-2154.

Sarafian, A.R., Marschall, H.R., Nielsen, S.G., McCubbin, F.M., Monteleone, B. (2014) An Earth-like hydrogen isotopic composition of Vesta as revealed by apatites. 45th Lunar Planet. Sci. abstract #2106.

Savage, P. and Moynier, F. (2013) Silicon isotopic variations in enstatite meteorites: Clues to their origin and Earth forming materials. Earth Planet. Sci. Lett. 361: 487-496.

Schaefer, L. and Fegley, B., Jr. (2007) Outgassing of ordinary chondritic material and some of its implications for the chemistry of asteroids, planets, and satellites. Icarus 186, 462-483.

Schaefer, L. and Fegley, B., Jr. (2010) Volatile element chemistry during metamorphism of ordinary chondritic material and some of its implications for the composition of asteroids. Icarus 205, 483-496.

Schaefer, L. and Fegley, B., Jr. (2010b) Cosmochemistry. pp. 347-377, In *Principles and Perspectives in Cosmochemistry: Lecture Notes of the Kodai School on "Synthesis of Elements in Stars"* (eds. A. Goswami and B. E. Reddy), Springer.

Schiller M., Baker J., Creech J., et al. (2011) Rapid timescales for magma ocean crystallization on the howardite-eucrite-diogenite parent body. Astrophys. J.740, L22.

Schiller, M., Paton, Bizzarro, M. (2012) Calcium isotope measurements by combined HR-ICP-MS and TIMS. JAAS, DOI: 10.1039/c1ja10272a

Simon J., DePaolo D.J., Moynier F. (2009) Calcium isotope composition of meteorites, Earth, and Mars, Astrophys. J. 702, 707-715.

Simon, J.I. and DePaolo, D.J., (2010) Stable calcium isotopic composition of meteorites and rocky planets. Earth Planet. Sci. Lett. 289, 457-466.

Slattery, W. L. (1978) Protoplanetary core formation by rain-out of iron drops. Moon Planets 19, 443-457.

Slattery, W. L., DeCampli, W. M., and Cameron, A. G. W. (1980) Protoplanetary core formation by rain-out of minerals. Moon Planets 23, 381-390.

Sprung, P., Scherer, E. E., Upadhyay, D., Leya, I., Mezger, K. (2010) Non-nucleosynthetic heterogeneity in non-radiogenic stable Hf isotopes: Implications for early solar system chronology. Earth Planet. Sci. Lett. 295, 1-11

Suess, H. E. and Urey, H. C. (1956) Abundances of the elements. Rev. Mod. Phys. 28, 53-74.

Steele, R.C.J., Coath, C.D., Regelous, M., Russell, S., Elliott, T. (2012) Neutron-poor nickel isotope anomalies in meteorites. Astrophys. J. 758, 59

Tang H., and Dauphas N. (2012) Abundance, distribution, and origin of ^{60}Fe in the solar protoplanetary disk. Earth Planet. Sci. Lett. 359-360 , 248-263.

Teng, F.-Z., Wadhwa, M., Helz, R.T. (2007) Investigation of magnesium isotope fractionation during basalt differentiation: implications for a chondritic composition of the terrestrial mantle. Earth Planet. Sci. Lett. 261, 84–92.

Thiemens, M.H. (1999) Mass-independent isotope effects in planetary atmospheres and the early Solar System. Science. 283, 341-345.

Torgersen, T. (1989) Terrestrial helium degassing fluxes and the atmospheric helium budget: Implications with respect to the degassing processes of continental crust. Chem. Geol. 79, 1–14.

Trinquier A, Birck J-L, Allegre CJ, Gopel CJ, and Ulfbeck D (2008) ^{53}Mn ^{53}Cr systematics of the early solar system revisited. Geochim. Cosmochim. Acta 72, 5146–5163.

Trinquier, A., Elliott, T., Ulfbeck, D., Coath, C., Krot, A.N., Bizzarro, M. (2009) Origin of nucleosynthetic isotope heterogeneity in the solar protoplanetary disk. Science. 324, 374-376.

Valdes, M., Moreira, M., Foriel, J., Moynier, F. (2014) The nature of the Earth's building blocks as revealed by calcium isotopes. Earth Planet. Sci. Lett. 394, 135-145.

Wadhwa M, Amelin Y, Bogdanovski O, Shukolyukov A, Lugmair GW, and Janney P (2009) Ancient relative and absolute ages for a basaltic meteorite: Implications for timescales of planetesimals accretion and differentiation. Geochim. Cosmochim. Acta 73, 5189–5201.

Wang, K., Moynier, F., Podosek, F., Foriel, J. (2011) ^{58}Fe and ^{54}Cr in early Solar System materials. Astrophys. J. Lett. 738, L58.

Wänke, H. (1981) Constitution of terrestrial planets. Phil. Trans. Roy. Soc. London A303, 287-302.

Wänke H, Dreibus G, and Jagoutz E (1984) Mantle chemistry and accretion history of the Earth. In: Kröner A (ed.) Archean Geochemistry. Berlin: Springer Verlag.

Warren, P. (2011) Stable isotopic anomalies and the accretionary assemblage of the Earth and Mars: A subordinate role of Carbonaceous chondrites, Earth Planet. Sci let. 311, 93-100

Wilkening, L. L. (1977) Meteorites in meteorites – Evidence for mixing among the asteroids. In Comets, Asteroids, Meteorites (ed. A.H. Delsemme), pp. 389-396, Univ. Toledo Press, Toledo, OH.

Yin, Q., Jacobsen, S. B. , Yamashita, K., Blichert-Toft. J., Télouk, P., Albarède, F. Yokoyama (2007) A short timescale for terrestrial planet formation from Hf-W chronometry of meteorites. Nature. 418, 949-952.

Zhang, Y. (2014) Degassing history of the Earth. Chapter 6.2 in Treatise on Geochemistry 2nd ed. Elsevier.

Zhang J, Dauphas N. , Davis A.M., Leya I., Fedkin A. 2012. The proto-Earth as a significant source of lunar material. Nature Geos. 5 , 251-255.

Figure captions

Figure 1. Chemical equilibrium abundances of stable condensates in the solar nebula as a function of inverse radial distance (AU^{-1}) along an adiabatic P – T profile. The condensate abundances are the logarithm of each condensate partial pressure (in bar) if the condensate were vaporized to a molecular gas of the same composition (see the mineral/formula key). The average orbital distances of the terrestrial

planets Mercury, Venus, Earth, and Mars are indicated by their astrological symbols along the bottom of the figure. This figure shows the higher temperature region and Figure 2 shows the lower temperature region of the inner solar nebula. Reproduced from Barshay (1981) with the permission of Dr. Barshay.

Figure 2. Chemical equilibrium abundances of stable condensates in the solar nebula as a function of inverse radial distance (AU^{-1}) along an adiabatic P – T profile. The abbreviation F/N is used where the abundances of feldspar and nepheline are subequal. The total pressure curve gives 10^{-4} times the total pressure at any temperature, e.g., 10^{-4} bar at 600 K. Reproduced from Barshay (1981) with the permission of Dr. Barshay.

Figure 3. The computed mean atomic mass (amu) as a function of inverse radial distance (AU^{-1}) for square wave accretion functions of variable width (see text). The shape of the square wave accretion function used to generate each curve is drawn to scale and its width is given. The present orbits of the terrestrial planets Mercury, Venus, Earth, and Mars are marked with their astrological symbols along the horizontal scale. Reproduced from Barshay (1981) with Dr. Barshay's permission.

Figure 4. The computed mean atomic mass (amu) as a function of inverse radial distance (AU^{-1}) for triangular accretion functions of variable width (see text). The shape of the triangular accretion function used to generate each curve is drawn to scale and its full width at half maximum (FWHM) is given. The present orbits of the

terrestrial planets Mercury, Venus, Earth, and Mars are marked with their astrological symbols along the horizontal scale. Reproduced from Barshay (1981) with Dr. Barshay's permission.

Figure 5. The computed mean atomic mass (amu) as a function of inverse radial distance (AU^{-1}) for Gaussian accretion functions of variable width (see text). The shape of the triangular accretion function used to generate each curve is drawn to scale and its full width at half maximum (FWHM) is given. The wings of the Gaussian accretion functions are drawn out as far as the distance at which ~ 0.1% of the available mass is accreted into the planet. The present orbits of the terrestrial planets Mercury, Venus, Earth, and Mars are marked with their astrological symbols along the horizontal scale. Reproduced from Barshay (1981) with Dr. Barshay's permission.

Figure 6. Isotopic anomalies for elements which show difference between different meteorite groups. $\Delta^{17}O=\delta^{17}O-0.52\delta^{18}O$. The $\varepsilon^{a}X_{b/c}$ corresponds to the per ten thousand deviation of the ratio $^{a}X/^{c}X$ internally normalized to the $^{c}X/^{c}X$ ratio (see main text for details). Data are from Clayton and Mayeda (1996, 1999), Clayton and Mayeda (1991), Burkhardt et al. (2011), Chen et al. (2010), Zhang et al. (2012), Trinquier et al. (2009), Moynier et al. (2012), Steele et al. (2012).

Figure 7. Ca isotope composition of various group of meteorites measured by different groups. The data are reported as the permil deviation of the $^{44}Ca/^{40}Ca$ ratio compared to the SRM914a standard. Contrary to previously proposed, E chondrites have very similar Ca isotope composition with terrestrial rocks (such are ordinary chondrites, and CO chondrites). Data are from Valdes et al. (2014), Simon and DePaolo (2010), Schiller et al. (2012) and Huang and Jacobsen (2011, 2012).

Figure 1:

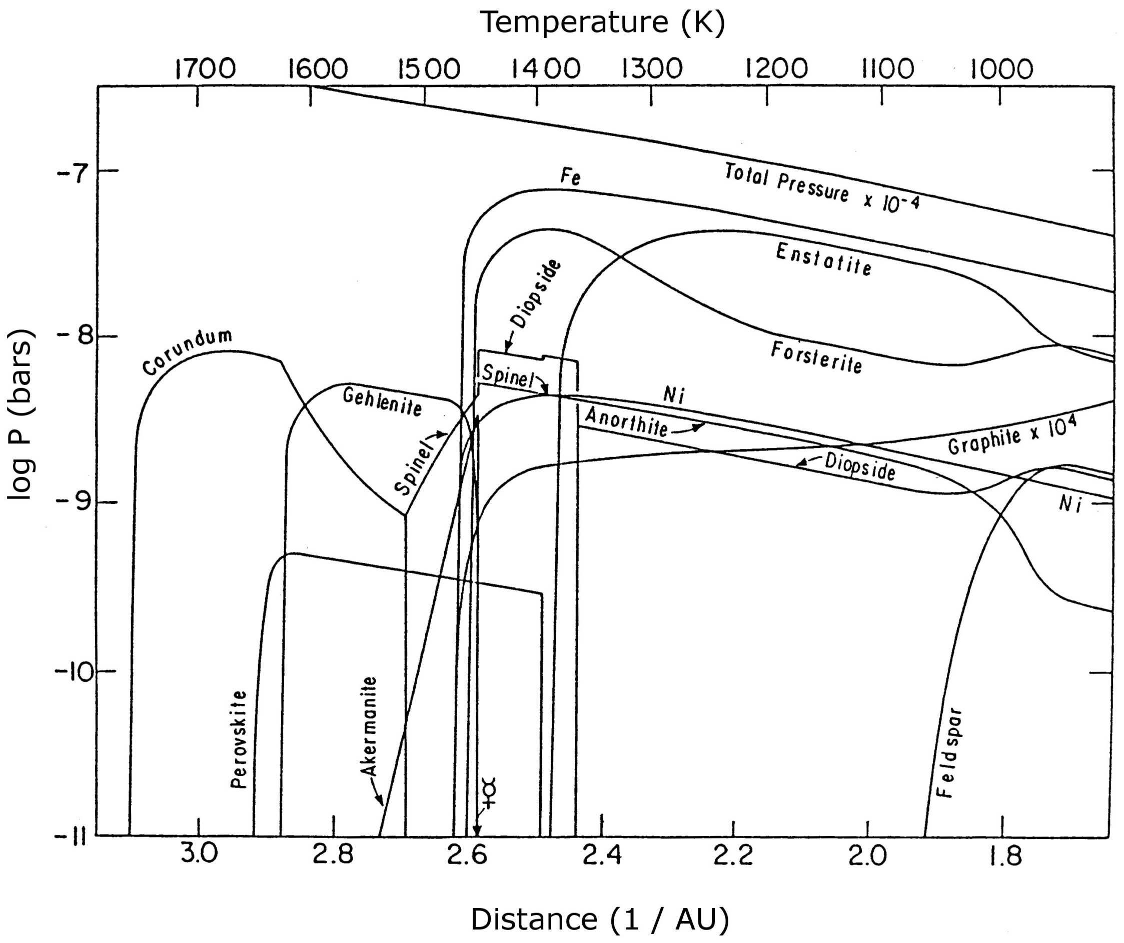
Temperature (K)
1700
1600
1500
1400
1300
1200
1100
1000
log P (bars)
-7
-8
-9
-10
-11
Total Pressure x 10^{-4}
Fe
Enstatite
Diopside
Forsterite
Corundum
Gehlenite
Spinel
Spinel
Ni
Anorthite
Graphite x 10^4
Diopside
Ni
Perovskite
Akermanite
☿
Feldspar
3.0
2.8
2.6
2.4
2.2
2.0
1.8
Distance (1 / AU)

Figure 2:

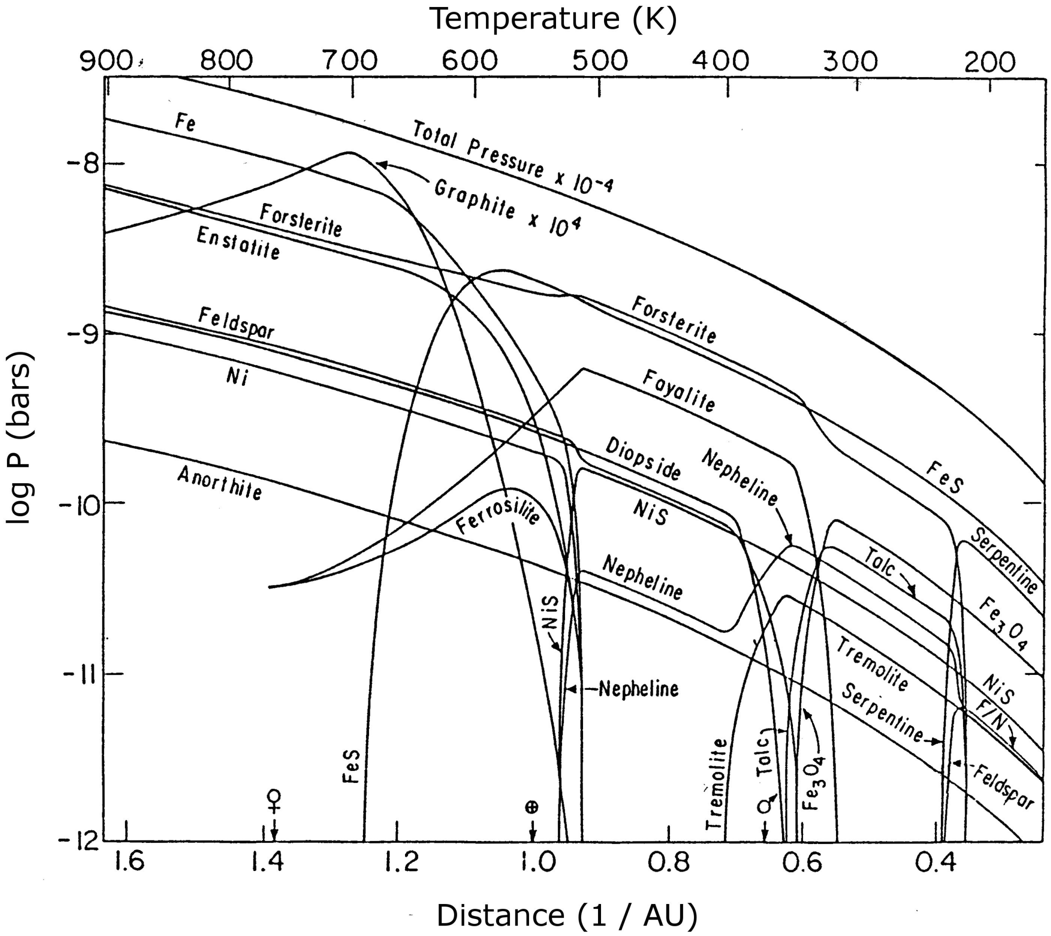
Temperature (K)
900
800
700
600
500
400
300
200
log P (bars)
-8
-9
-10
-11
-12
Distance (1 / AU)
1.6
1.4
1.2
1.0
0.8
0.6
0.4
Fe
Total Pressure x 10^{-4}
Graphite x 10^4
Forsterite
Enstatite
Forsterite
Feldspar
Ni
Fayalite
Diopside
Nepheline
Anorthite
Ferrosilite
NiS
Nepheline
FeS
Serpentine
Talc
Fe_3O_4
Tremolite
NiS
F/N
Serpentine
Feldspar
NiS
Nepheline
FeS
Tremolite
Talc
Fe_3O_4
♀
⊕
♂

Figure 3

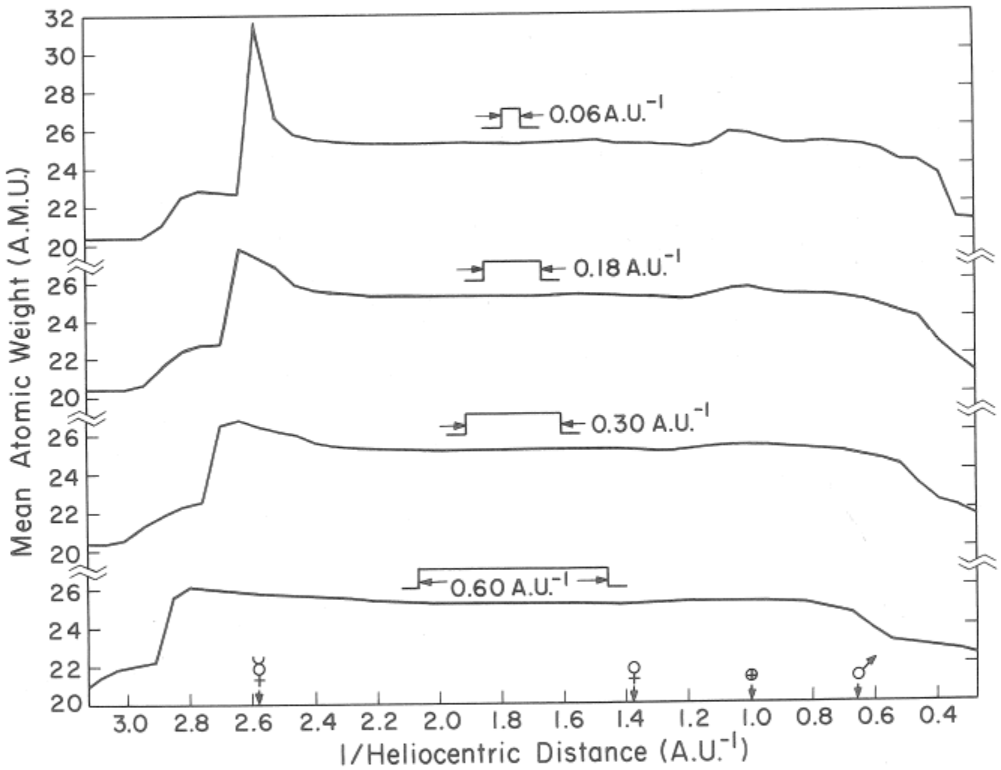
Mean Atomic Weight (A.M.U.)
32
30
28
26
24
22
20
0.06 A.U.$^{-1}$
0.18 A.U.$^{-1}$
0.30 A.U.$^{-1}$
0.60 A.U.$^{-1}$
☿
♀
⊕
♂
3.0
2.8
2.6
2.4
2.2
2.0
1.8
1.6
1.4
1.2
1.0
0.8
0.6
0.4
1/Heliocentric Distance (A.U.$^{-1}$)

Figure 4:

Figure 4

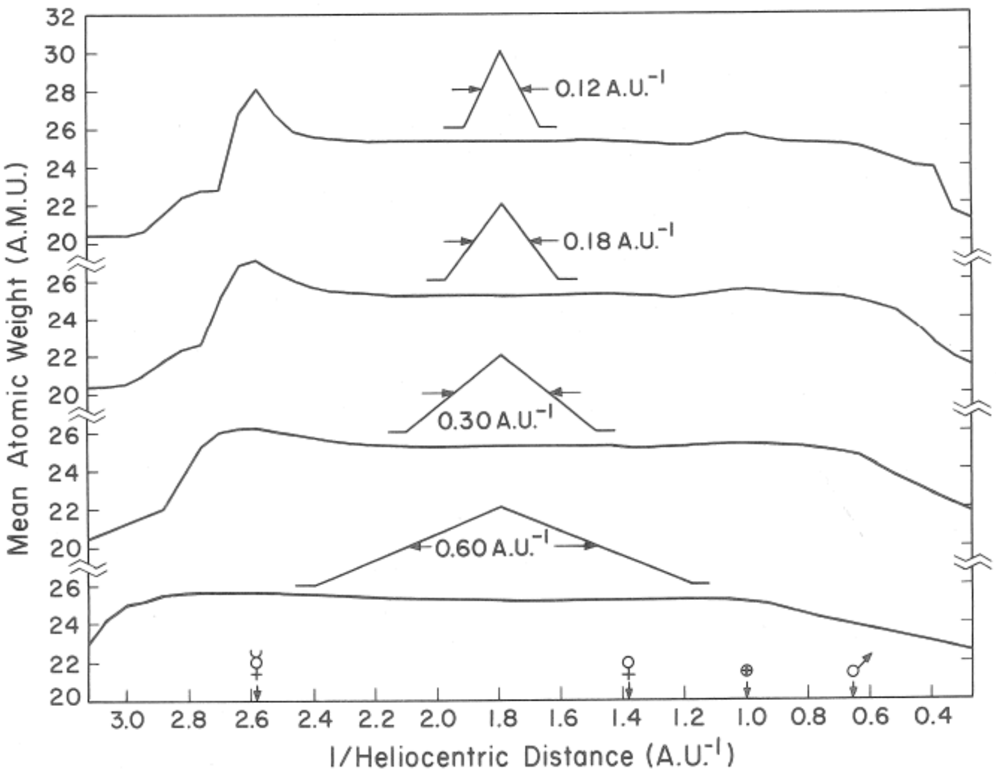

Figure 5:

Figure 5

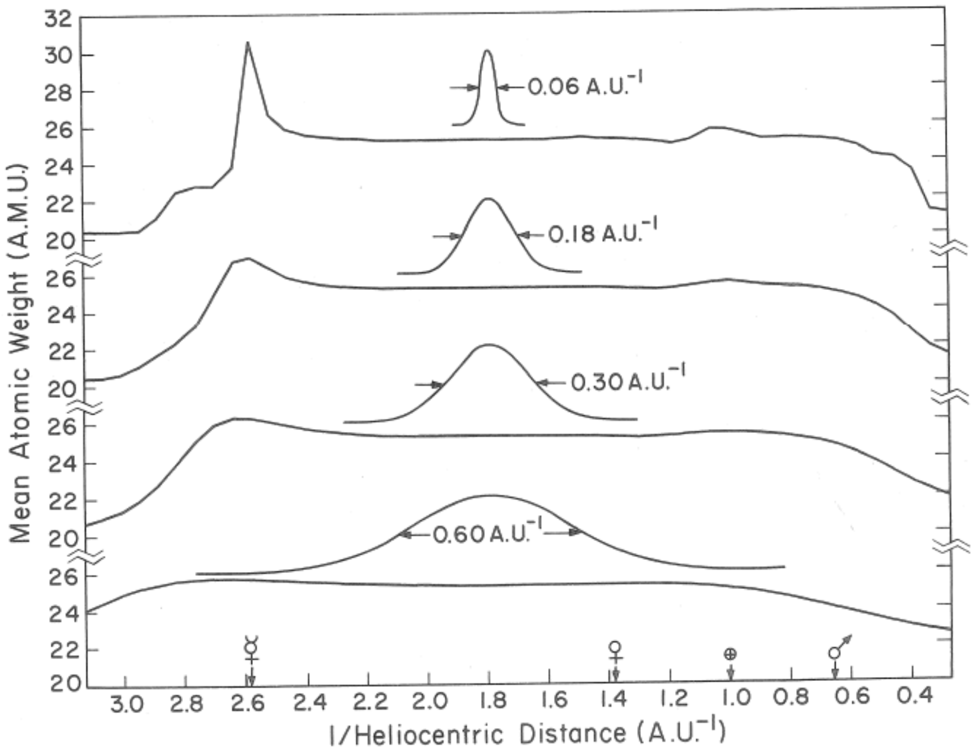

Figure 6:

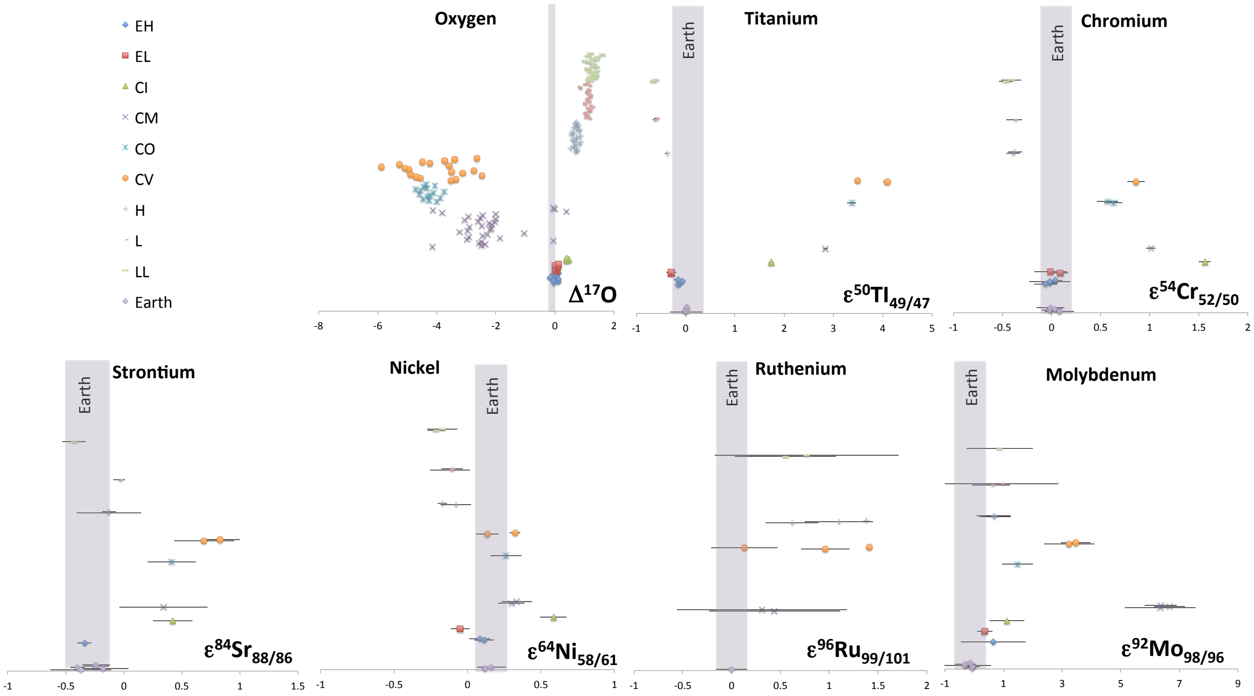
EH
EL
CI
CM
CO
CV
H
L
LL
Earth
Oxygen
$\Delta^{17}O$
-8
-6
-4
-2
0
2
Titanium
Earth
$\varepsilon^{50}Ti_{49/47}$
-1
0
1
2
3
4
5
Chromium
Earth
$\varepsilon^{54}Cr_{52/50}$
-1
-0.5
0
0.5
1
1.5
2
Strontium
Earth
$\varepsilon^{84}Sr_{88/86}$
-1
-0.5
0
0.5
1
1.5
Nickel
Earth
$\varepsilon^{64}Ni_{58/61}$
-1
-0.5
0
0.5
1
Ruthenium
Earth
$\varepsilon^{96}Ru_{99/101}$
-1
-0.5
0
0.5
1
1.5
2
Molybdenum
Earth
$\varepsilon^{92}Mo_{98/96}$
-1
1
3
5
7
9

Figure 7:

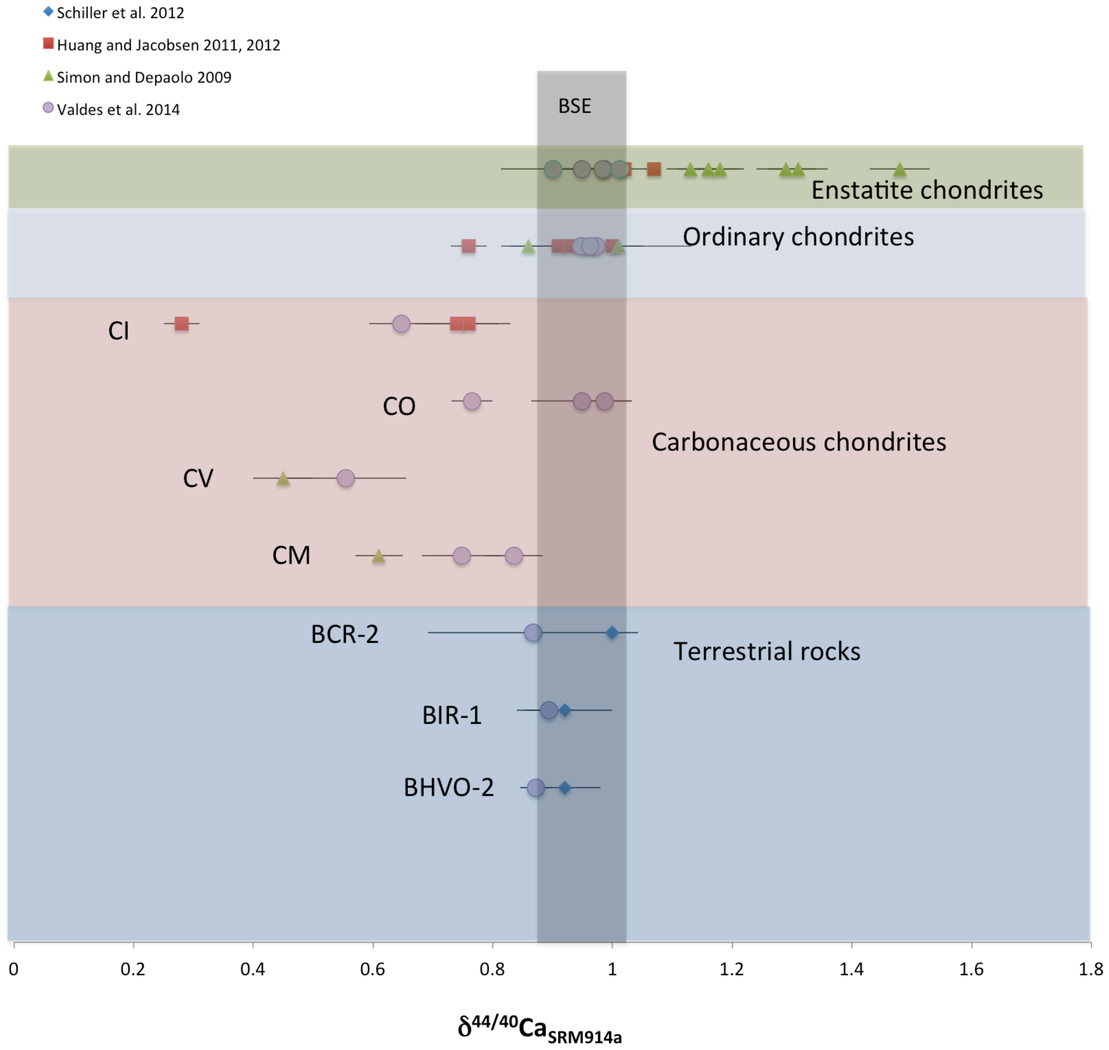

Schiller et al. 2012
Huang and Jacobsen 2011, 2012
Simon and Depaolo 2009
Valdes et al. 2014
BSE
Enstatite chondrites
Ordinary chondrites
CI
CO
Carbonaceous chondrites
CV
CM
BCR-2
Terrestrial rocks
BIR-1
BHVO-2
0
0.2
0.4
0.6
0.8
1
1.2
1.4
1.6
1.8
$\delta^{44/40}Ca_{SRM914a}$

Table 1 Earth's geochemical reservoirs[a]

		Mass Fractions	
Reservoir	Mass (kg)	of Bulk Silicate Earth[b]	of Total Earth
Total Atmosphere	**5.137×10^{18}**	**1.27×10^{-6}**	**8.60×10^{-7}**
Troposphere	4.22×10^{18}	1.05×10^{-6}	7.06×10^{-7}
Stratosphere	0.906×10^{18}	2.25×10^{-7}	1.52×10^{-7}
Upper Atmosphere	4×10^{15}	9.9×10^{-10}	6.7×10^{-10}
Biosphere	**1.148×10^{16}**	**2.85×10^{-9}**	**1.92×10^{-9}**
Hydrosphere	**1.664×10^{21}**	**4.13×10^{-4}**	**2.79×10^{-4}**
Total petrosphere[c]	**4.031×10^{24}**	**0.9995**	**0.6748**
Continental Crust	1.522×10^{22}	3.77×10^{-3}	2.55×10^{-3}
Oceanic Crust	0.845×10^{22}	2.10×10^{-3}	1.41×10^{-3}
Total Crust	2.367×10^{22}	5.87×10^{-3}	3.96×10^{-3}
Upper Mantle	1.068×10^{24}	0.2648	0.1788
Lower Mantle	2.939×10^{24}	0.7287	0.4920
Total Mantle	4.007×10^{24}	0.9936	0.6708
Total Core	**1.941×10^{24}**	**–**	**0.3249**
Outer Core	1.839×10^{24}	–	0.3078
Inner Core	0.102×10^{24}	–	0.0171
Entire Earth	**5.9736×10^{24}**		**1.0000**

[a] Modified from K. Lodders and B. Fegley "The Planetary Scientist's Companion," Oxford, New York, NY, 1998.

[b] Total mass of the bulk silicate Earth (BSE) is 4.033×10^{24} kg.

[c] We define lithosphere as the silicate portion of the BSE, i.e., crust + entire mantle.

Table 2 Bulk Earth Compositional Models (ppm by mass or mass %)[a]

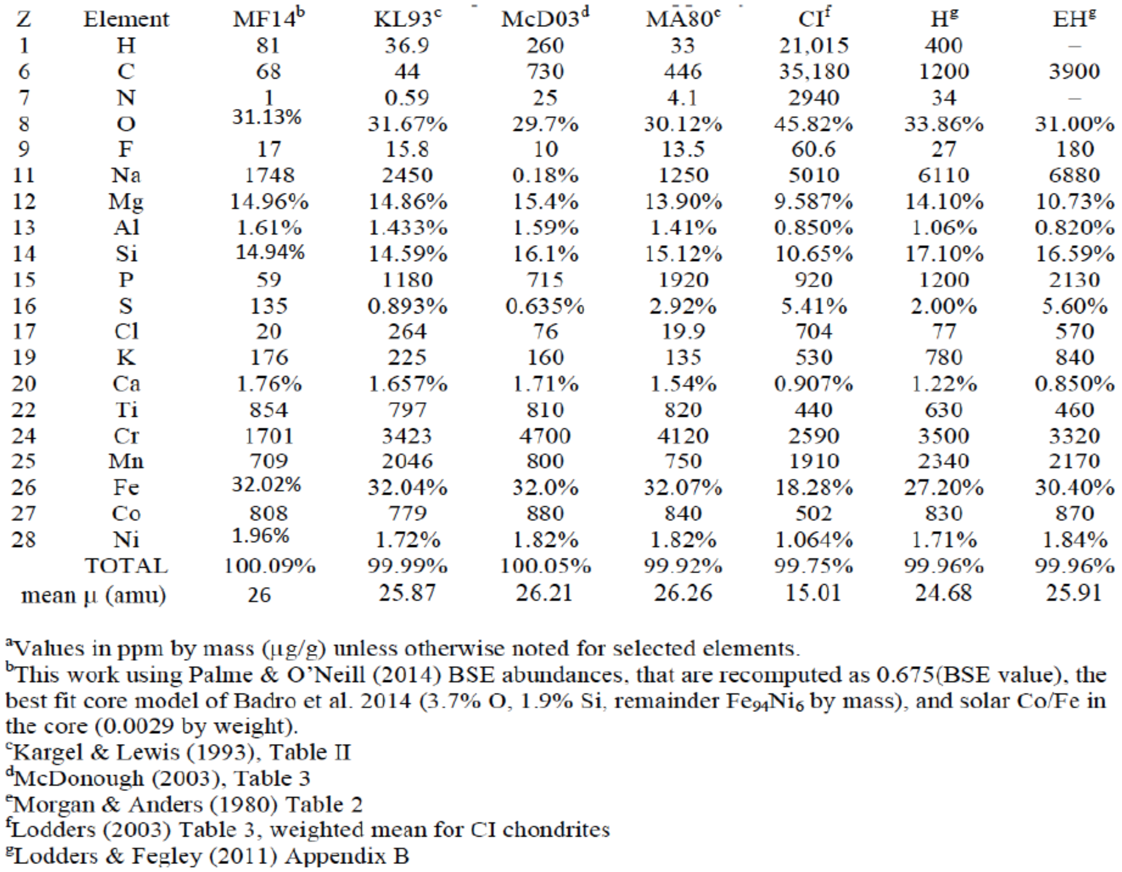

Z	Element	MF14[b]	KL93[c]	McD03[d]	MA80[e]	CI[f]	H[g]	EH[g]
1	H	81	36.9	260	33	21,015	400	–
6	C	68	44	730	446	35,180	1200	3900
7	N	1	0.59	25	4.1	2940	34	–
8	O	31.13%	31.67%	29.7%	30.12%	45.82%	33.86%	31.00%
9	F	17	15.8	10	13.5	60.6	27	180
11	Na	1748	2450	0.18%	1250	5010	6110	6880
12	Mg	14.96%	14.86%	15.4%	13.90%	9.587%	14.10%	10.73%
13	Al	1.61%	1.433%	1.59%	1.41%	0.850%	1.06%	0.820%
14	Si	14.94%	14.59%	16.1%	15.12%	10.65%	17.10%	16.59%
15	P	59	1180	715	1920	920	1200	2130
16	S	135	0.893%	0.635%	2.92%	5.41%	2.00%	5.60%
17	Cl	20	264	76	19.9	704	77	570
19	K	176	225	160	135	530	780	840
20	Ca	1.76%	1.657%	1.71%	1.54%	0.907%	1.22%	0.850%
22	Ti	854	797	810	820	440	630	460
24	Cr	1701	3423	4700	4120	2590	3500	3320
25	Mn	709	2046	800	750	1910	2340	2170
26	Fe	32.02%	32.04%	32.0%	32.07%	18.28%	27.20%	30.40%
27	Co	808	779	880	840	502	830	870
28	Ni	1.96%	1.72%	1.82%	1.82%	1.064%	1.71%	1.84%
	TOTAL	100.09%	99.99%	100.05%	99.92%	99.75%	99.96%	99.96%
mean μ (amu)		26	25.87	26.21	26.26	15.01	24.68	25.91

[a] Values in ppm by mass (μg/g) unless otherwise noted for selected elements.

[b] This work using Palme & O'Neill (2014) BSE abundances, that are recomputed as 0.675(BSE value), the best fit core model of Badro et al. 2014 (3.7% O, 1.9% Si, remainder $Fe_{94}Ni_6$ by mass), and solar Co/Fe in the core (0.0029 by weight).

[c] Kargel & Lewis (1993), Table II

[d] McDonough (2003), Table 3

[e] Morgan & Anders (1980) Table 2

[f] Lodders (2003) Table 3, weighted mean for CI chondrites

[g] Lodders & Fegley (2011) Appendix B

Table 3 Volatile elements in bulk silicate Earth, bulk silicate Vesta, and ordinary chondrites

Element	BSV (ppm)[a]	BSE (ppm)[b]	BSV/BSE	Chondrites[d]	BSE/chondrites
H	?	120	?	470	0.26
C[c]	10 – 30	100	0.1 – 0.3	2570	0.04
N[c]	0.05 – 1.3	2	0.025 – 0.65	54	0.04
Zn	0.36	53.5	0.0067	53.2	1.0
Na	757	2590	0.29	6950	0.37
K	66	260	0.25	860	0.30
Rb	0.06	0.605	0.10	2.1	0.29
Cs	0.002	0.018	0.11	0.06	0.30
F	4.8	25	0.19	38	0.66
Cl	4.6	30	0.15	93	0.32
Br	0.03	0.075	0.40	0.5	0.15

[a] BSV values are mainly from Dreibus & Wanke (1980) and Dreibus et al. (1997)

[b] BSE values are from Palme & O'Neill (2014)

[c] Carbon and nitrogen values for BSV are eucrite data from Grady & Wright (2003)

[d] Average ordinary chondrite data are from Schaefer & Fegley (2007, 2010)